



Optimal strategies for combining vaccine prioritization and social distancing to reduce hospitalizations and mitigate COVID19 progression

Sharon Guerstein¹, Victoria Romeo-Aznar², Ma'ayan Dekel¹, Oren Miron³, Nadav Davidovitch³, Rami Puzis ⁴, and Shai Pilosof ^{1,*}

¹*Department of Life Sciences, Ben-Gurion University of the Negev, Beer-Sheva, Israel*

²*Department of Ecology & Evolution, University of Chicago*

³*School of Public Health, Faculty of Health Sciences, Ben-Gurion University of the Negev, Beer-Sheva, Israel*

⁴*Software and Information Systems Engineering, Ben-Gurion University of the Negev*

* *Corresponding author: pilos@bgu.ac.il*

December 22, 2020

Abstract

Social distancing is an effective population-level mitigation strategy to prevent COVID19 propagation but it does not reduce the number of susceptible individuals and bears severe economic and psychological consequences. A vaccine has recently been developed but its deployment will be limited and not immediate. Designing an optimal combination of these two intervention strategies is a priority, but a mechanistic understanding of the interplay between these strategies is missing. To tackle this challenge we developed an age-structured deterministic model in which vaccines are deployed during the pandemic to individuals who, in the eye of public health, are susceptible (do not show symptoms). The model allows for flexible and dynamic prioritization strategies with shifts between target groups. We find that social distancing applied uniformly to all ages and with vaccination targeted towards adults (20-59) or elderly (60+) work in synergism but up to a threshold beyond which vaccination is not efficient. The inefficiency threshold can be eliminated by targeting social distancing at the age groups that are not vaccinated and the optimal strategy is to prioritize vaccines to elderly. Nevertheless, while vaccination reduces hospitalizations, it does not affect the time it takes to eliminate the virus from the population, which is affected only by social distancing. Finally, the same reduction in hospitalization can be achieved via different combination of strategies, giving decision makers flexibility in choosing public health policies. Our study provides insights into the factors that affect vaccination success and provides methodology to test different intervention strategies in a way that will align with ethical guidelines.

Introduction

Vaccines are an essential tool for reducing, or even eliminating the burden of endemic diseases, such as measles, hepatitis, and influenza. For such diseases, vaccine development and production is, by now, a well-practiced process. Nevertheless, developing, producing, and deploying vaccines in the midst of a pandemic is a great challenge. For example, during the H1N1 pandemic vaccines were limited and their deployment required prioritization [1]. COVID19 is a typical example of such a situation. Without vaccines, the only strategy to contain COVID19 is to cut transmission chains by reducing contacts. Public health measures such as social distancing, improved hygiene, and face masks effectively reduce the risk of infection but do not reduce susceptibility among the population. Moreover, social-distancing interventions also bear social, economic, and psychological consequences [2, 3]. Therefore, vaccine development for COVID19 has been carried out at an unprecedented pace. Nevertheless, even now, when a vaccine is available, its deployment requires prioritization due to high demand and low supply. Thinking ahead about relevant strategies for deployment may save not only valuable time for policy makers [1, 4], but eventually lives and it is therefore at the forefront of debate and research [5–9].

A recent modeling study [10] examined several age-dependent vaccine prioritization strategies with a varying vaccine efficacy. One crucial result was that vaccinating adults at the ages of 60+ reduced mortality more than other vaccination strategies (e.g., vaccinating juveniles) for a non-leaky vaccine. In this SEIR model, a certain proportion of the population was selected and vaccinated before the onset of disease. In reality, however, vaccines are deployed to parts of the population during the pandemic, with some prioritization strategy. Another crucial aspect to consider is social-distancing because a major driving force of the COVID19 disease is asymptomatic infections. When a vaccine is deployed, social-distancing is still enforced

at some level, possibly on some age groups more than on others. Jentsch et al [11] presented an evolutionary game model that combined non-adherence to non-pharmaceutical interventions (lockdown, masks) and vaccination but did not explicitly test for the optimal combination of these two strategies. *The question is therefore how to combine vaccines with social distancing in the most efficient way?*

Here, we use a data-driven, age-structured, deterministic model to examine combinations of vaccine deployment and social distancing and the interaction between them. Our model is flexible and novel for several reasons. First, it contains, beyond an age structure and age-dependent contact matrices, an asymptomatic state and a quarantined state for symptomatic individuals. Second, vaccination dynamics reflect real-world scenarios because vaccines are deployed to individuals who, in the eye of public health, are susceptible: asymptomatic (exposed and infectious), those that have recovered from an asymptomatic infection, and true susceptibles (those who were never infected). In addition, vaccines are deployed after the onset of the pandemic. The model also allows for flexible prioritization strategies: One can choose a certain order of age groups to vaccinate, and if the number of individuals to vaccinate at a certain group is depleted but there are still vaccines available, the model shifts dynamically to the next group. Finally, it allows modeling a combined implementation of both social distancing and vaccination.

Our goal is to illuminate qualitative effects of the combination of vaccine deployment and social distancing strategies on COVID-19 progression. We focus on reduction in hospitalizations because hospital care is a limited resource in public health, which is also correlated with mortality. We show that a combination of vaccination and social distancing has a synergistic effect, but up to a certain threshold of social distancing above which vaccination is no longer effective. This threshold can be eliminated for efficient synergism if social distancing is targeted at the non-vaccinated group. Moreover, the same reduction in hospitalization can be achieved via different combination of strategies, giving decision makers flexibility in choosing public health policies. These results were consistent for six countries.

Results

We developed an age-structured deterministic compartmental model that reflects the main states of COVID19 progression (Fig. 1). We used 10-yr interval age-grouping (0-9, 10-19,...,70-79,80+), in line with previous studies of COVID19 (e.g, [12]) and with the data management protocols of most countries. Vaccines are deployed at a constant rate of κ vaccines per day, which we measure as the percentage of population that a government can vaccinate a day. The amount of daily vaccines is divided equally across the target age groups. For example, if the strategy is to vaccinate adults 60+, then each of the age groups 60-69, 70-79 and 80+ will get $\mu_j = \kappa/3$ vaccines. The model allows for dynamic prioritization by selecting an order of preferred target age groups and moving from one to the next when there are no individuals left to vaccinate at the current target group (Fig. 2). We run the model for 30 weeks (Fig. S1, S2). The model and choice of parameter values are detailed in the Methods.

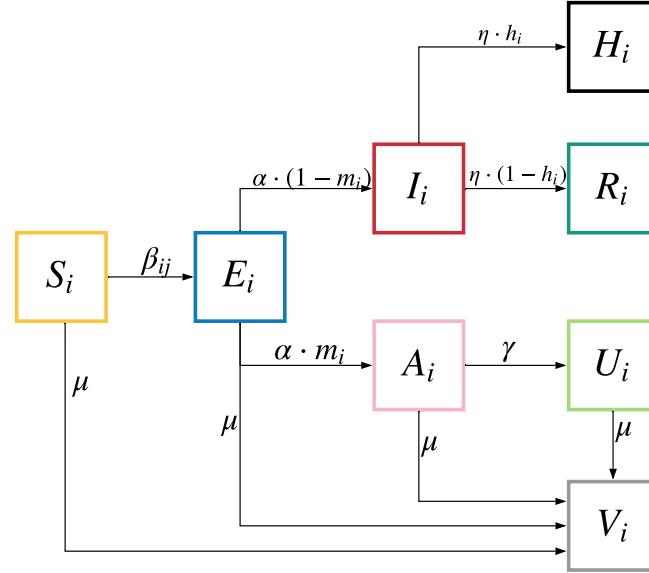


Figure 1: Model description. Individuals transition between states with rates specified by Greek letters. Small Latin letters are probabilities. Subscripts j and l depict age groups. Individuals start at a susceptible state (S) and upon infection with an age-dependent rate β_{lj} become infected with the virus (E). After an incubation period of $1/\alpha$ days individuals become either asymptomatic (A) with a probability m_j or symptomatic (I). Symptomatic individuals are identified and removed to quarantine (R) within η days or, with a given probability h_j develop severe symptoms and go to the hospital (H). Asymptomatic individuals naturally recover (U) within γ days. All individuals that do not show symptoms can get a vaccine (V) at a constant rate of μ_j vaccines per day. See Methods for a comprehensive description of the model and parameters. Running the model without vaccination and starting with a single infected individual, we obtained similar disease dynamics as those observed in empirical data (Fig. S4).

We measure the effectiveness of a vaccine as the percent of reduction in hospitalizations compared to a no-vaccination scenario within each age group as

$$F_H^j = 1 - \frac{H_\kappa^j}{H_{\kappa=0}^j}, \quad (1)$$

where H_κ^j is the total number of hospitalizations in age group j for a given deployment rate κ , and $H_{\kappa=0}^j$ is the total number of hospitalizations in age group j when a vaccine is not deployed (Fig. 2). A similar measure can be used to calculate the effectiveness of a vaccine in reducing hospitalizations across all age groups:

$$F_H^{tot} = 1 - \frac{\sum_j H_\kappa^j}{\sum_j H_{\kappa=0}^j}. \quad (2)$$

It is made available under a [CC-BY-NC-ND 4.0 International license](https://creativecommons.org/licenses/by-nc-nd/4.0/) .

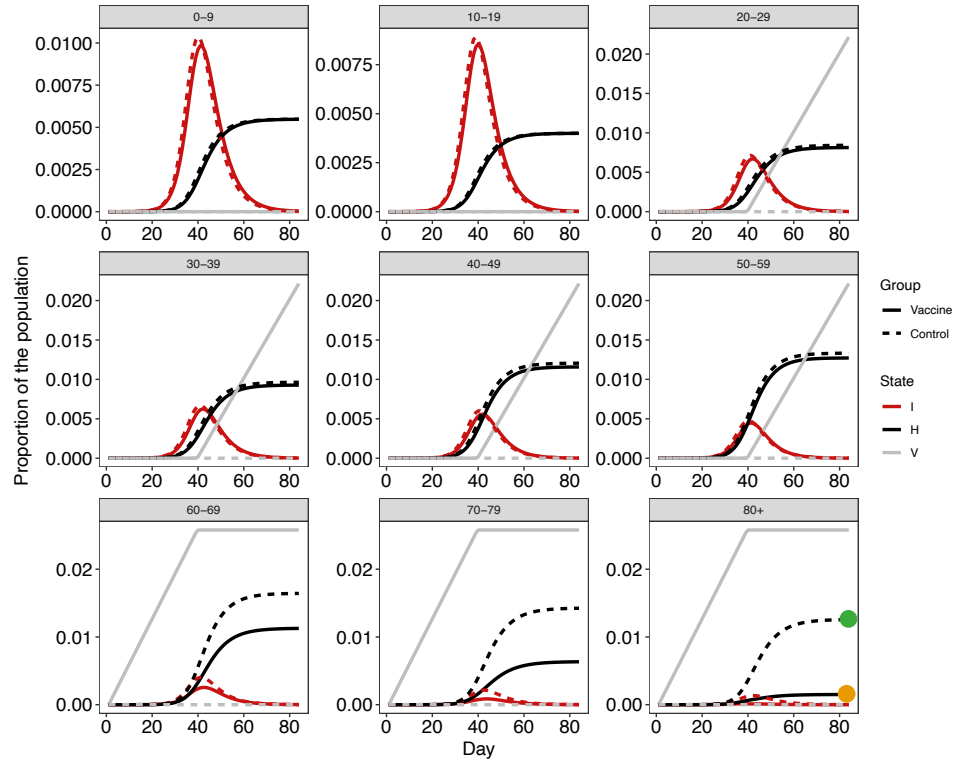


Figure 2: Model dynamics example. The model follows a population divided to nine age groups as depicted in the figure. Dashed lines depict control (no vaccine). Solid lines depict a strategy in which we first vaccinate elderly (60+) and then adults (20-59). In this example we use a single value of $\kappa = 0.2$ (0.2% of the population is vaccinated per day) and there is no social distancing. Around 40 days there are no more elderly to vaccinate and the model shifts to vaccinating adults (gray solid line). It is clear that most of the reduction in hospitalizations is obtained for the elderly groups (compare dashed to solid black lines). The orange and green dots mark the $H_{\kappa=0.2}^j$ and $H_{\kappa=0}^j$ values (for $j = 80+$) used in equation 1, respectively. Model was run for 30 weeks S2) but 12 weeks are plotted here for clarity. I : infectious and symptomatic (red); H : hospitalized (black); V : vaccinated (gray).

We present results in the main text for Israel, a small country of ≈ 8.7 million people, but we also tested our model using age demographics and contact matrices for Italy, Belgium, Finland, Germany, and Luxembourg and results were qualitatively the same for all countries, including Israel (Supplementary Information).

Vaccinating elderly is more effective than adults in reducing hospitalizations

As a benchmark, we first explore two vaccination strategies with no social distancing: (i) vaccinating all elderly (60+) and then all adults (20-59) and (ii) vaccinating all adults and then all elderly. Vaccines are currently not developed for children and we therefore did not include ages 0-19 in vaccination strategies. Because the proportion of elderly in the population is low, in the first strategy the switch to vaccinating adults occurs faster than the switch to vaccinating elderly in the second strategy (Fig. S5). F_H^{tot} is clearly greater for the first strategy (Fig. 3). It is important to note however that vaccinating a certain age group affects almost exclusively this age group alone (Fig. S6).

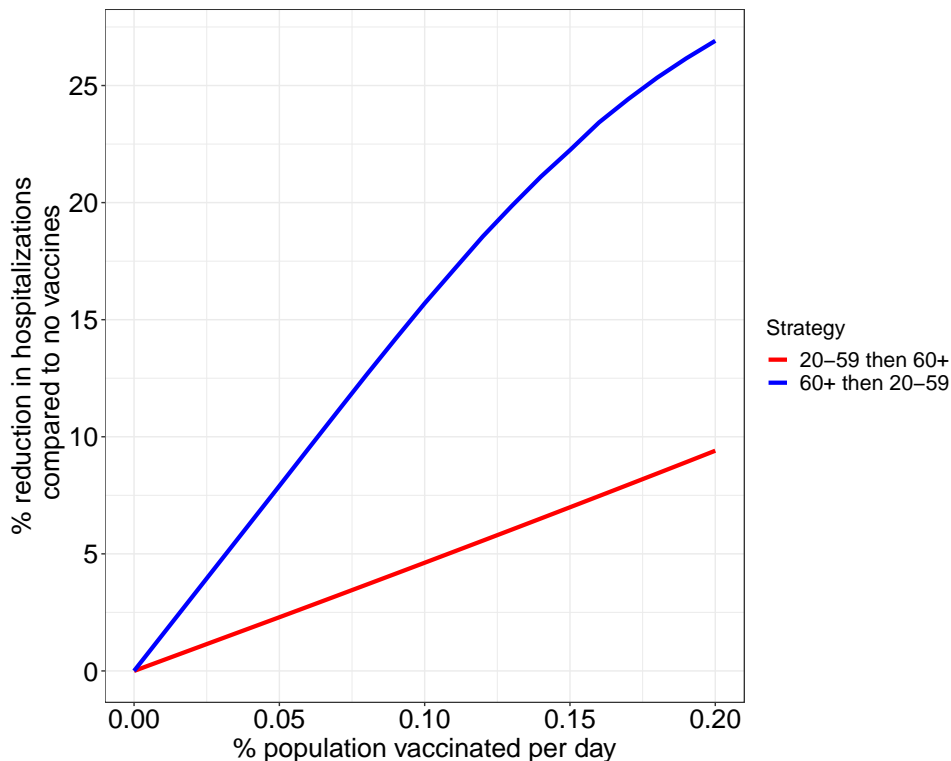


Figure 3: Comparison between prioritization strategies with no social distancing. The plot depicts the F_H^{tot} (y-axis) as a function of increasing vaccination rates (κ), measured as the proportion of the population vaccinated per day (e.g., $\kappa = 0.2$ translates to deployment of 16,000 vaccines per day in a population of 8 million people). Vaccinating elderly (60+) and then adults (20-59)—depicted in the blue line—is more effective than vaccinating adults and then elderly (red line).

A comparison to simulations in which the probability of hospitalizations is uniform across all age groups clearly shows that age-dependent disease severity underlies the increased reduction in hospitalizations obtained when vaccinating elderly first (Fig S7).

A threshold to the synergy between vaccination and uniform social distancing

Now that we have presented the two main prioritization strategies, we can address the main goal of this work: examining a combination of intervention measures. We test a scenario in which vaccines are deployed while social distancing is still in place – a highly likely scenario in every country. A combination of social distancing and vaccination is expected to have a synergistic, stronger effect in decreasing hospitalizations than any of these measures alone, and this effect should increase with stronger social distancing and higher vaccination rates. To test this hypothesis, we apply a uniform social distancing strategy by reducing contacts at the contact matrix by the same factor to all ages, including juveniles (see Methods).

As expected, the intervention measures work synergistically. However, there is a threshold of social distancing beyond which vaccination is no longer effective (F_H^{tot} decreases; Fig. 4). This threshold is a result of an overly-effective social distancing, which by itself prevents hospitalizations, overriding the need for vaccinations. Crucially, this does not mean that a vaccine is not necessary. Strong social distancing keeps the number of susceptible individuals high but without vaccine, individuals are bound to be infected.

The results also indicate that while vaccination is more effective when given to the elderly (higher F_H^{tot} for the same value of κ ; compare left to right panels in Fig. 4), F_H^{tot} increases faster with social distancing when adults are vaccinated. This is because adults are more connected in the social network and are therefore more affected by social distancing than the elderly.

An important observation is that the same level of efficiency in reducing hospitalizations (F_H^{tot}), can be obtained via different combinations of social distancing, vaccine prioritization and vaccine deployment rates. For example, a 30% efficiency (dotted line in Fig. 4) can be obtained by either: (i) vaccinating adults at a rate of 0.2% of the population per day with approximately 55% reduction in contacts; or (ii) vaccinating elderly at a rate of $\approx 0.1\%$ of the population per day with the same level of social distancing. This does not mean however that the same number of hospital beds can be spared as vaccine efficiency is measured compared to a no-vaccine control.

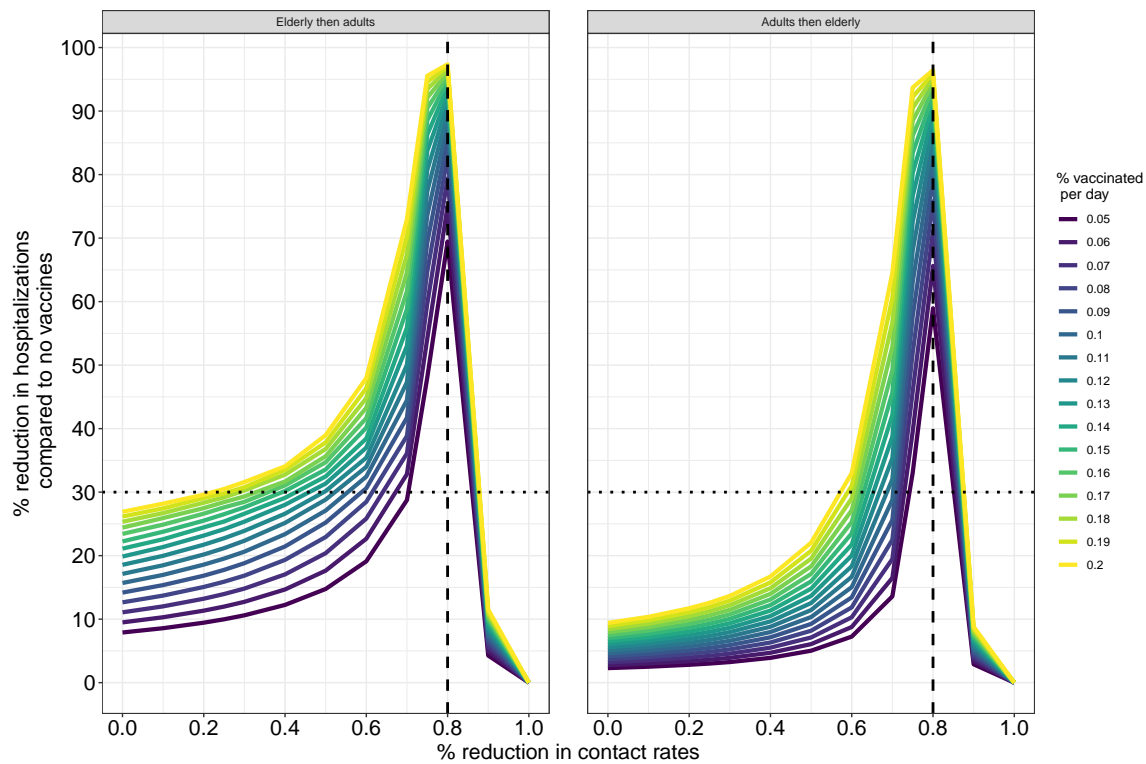


Figure 4: Comparison between prioritization strategies with uniform social distancing. The plot depicts the F_H^{tot} (y-axis) as a function of increasing social distancing (0: no social distancing; 1: no contacts). F_H^{tot} is calculated at the end of 30 weeks. Line colors depict κ , the proportion of the population vaccinated per day. Two strategies are shown: Vaccinating all elderly (60+) and then all adults (20-59) (left panel); and vaccinating adults and then elderly (right panel). In both strategies there is a threshold of reduction in contacts (dashed vertical line) above which vaccination is no longer effective. Horizontal dotted line provides an example of how the same level of vaccine efficiency (here, $F_H^{tot} = 0.3$) can be achieved using different combinations of social distancing, vaccine prioritization and vaccine deployment rates.

Targeted social distancing eliminates threshold in vaccine efficiency

One advantage of a vaccine is that it may provide a way to alleviate social distancing. We therefore modified our two strategies by applying social distancing only to the group that is not vaccinated: (i) vaccinating all

elderly (60+) and then all adults (20-59), while enforcing social distancing on adults (0-19 and 60+ maintain benchmark contact rates); and (ii) vaccinating all adults and then all elderly while enforcing social distancing on the elderly (0-59 maintain benchmark contact rates).

Targeted social distancing indeed eliminated the threshold but it also has dramatically different effects in both strategies. In this scenario, prioritizing vaccines to adults does not reduce hospitalizations as effectively as when prioritizing to elderly. Seemingly, the best strategy in reducing hospitalizations is prioritizing vaccines to elderly while applying social distancing to adults.

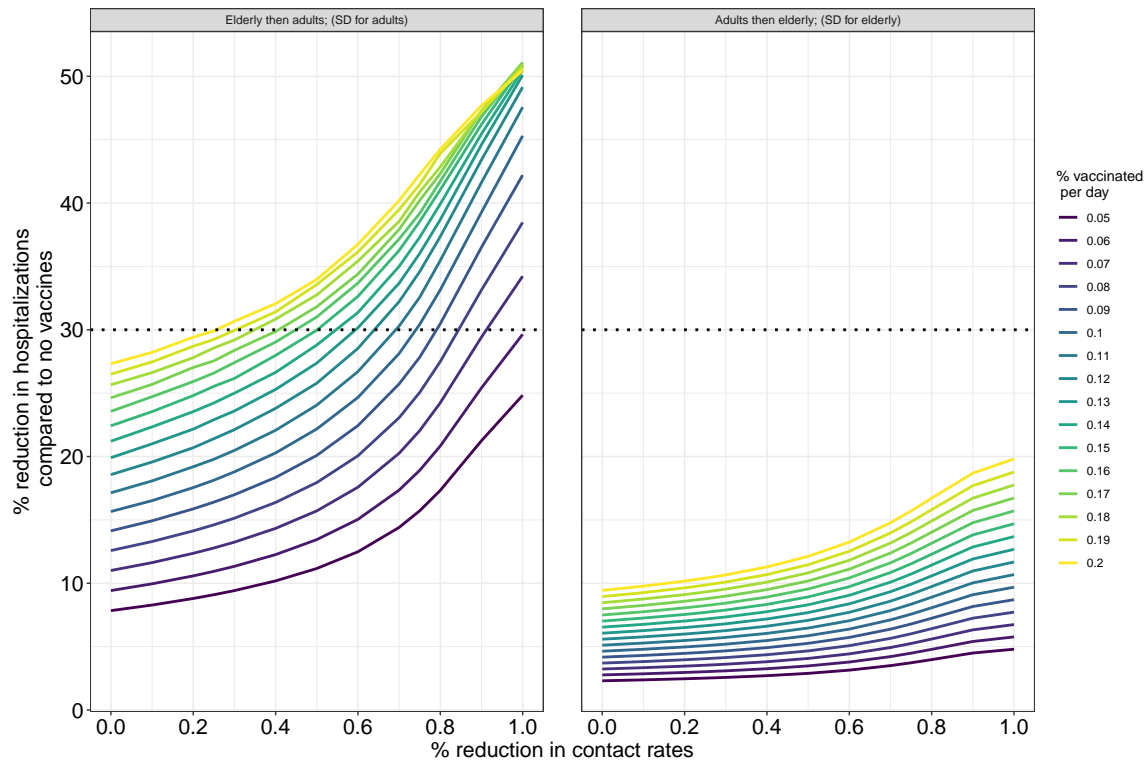


Figure 5: Comparison between prioritization strategies with targeted social distancing. The plot depicts the F_H^{tot} (y-axis) as a function of increasing social distancing (0: no social distancing; 1: no contacts). Line colors depict κ , the proportion of the population vaccinated per day. Two strategies are shown: Vaccinating all elderly (60+) and then all adults (20-59), while applying social distancing only in the adult group (left panel); and vaccinating adults and then elderly, while applying social distancing only in the elderly group (right panel). Horizontal dotted line at $F_H^{tot} = 0.3$ is the same as in Fig. 4. Vaccination has a minor effect on F_H^{tot} when prioritized to adults.

Time for virus elimination increases with social distancing, but is not affected by vaccination

Another important consideration when combining strategies is the time it takes to bring the number of infected cases to a level that would eliminate the disease. Typically, this is measured using R_0 . Nevertheless, regardless of how it is derived (e.g., using next-generation matrix), R_0 is defined as the average number of secondary cases at the beginning of the outbreak; that is, in a completely susceptible population. This is clearly not the case here and we therefore opted for two different approaches: (i) the percent of change in

the number of infected ($I + A$); and (ii) the time in which growth rate is $dI/dt + dA/dt \leq 0$. The two approaches showed that vaccination had little effect on the time it takes to eliminate the disease, but that increasing social distancing slowed the time to mitigation. We detail specific results for the former approach and present the later in the Supplementary Information.

Eliminating the disease requires a negative change in the percent of increase in infected and asymptomatic people (negative growth). We calculate this as $r_p = \frac{z_t - z_{t-1}}{z_{t-1}}$, where $z = I + A$. Under uniform social distancing, we find that the time to obtain $r_p = 0$ increases with social distancing in the same way as F_H^{tot} (Fig. 4) and is little affected by vaccination amount or strategy (Fig. 6). Social distancing increases the time to reach $r_p = 0$ because it prevents infections, keeping a larger pool of susceptible individuals for longer periods of time that the virus can infect. Once it reaches 0, however, r_p stays negative (Fig. S8). Under targeted social distancing, the time to reach $r_p = 0$ decreases considerably (see y-axis differences between upper and lower rows in Fig. 6) because more individuals are infected at the same amount of time (compared to uniform social distancing).

Overall, the results show that social distancing seems to be the only factor affecting virus growth and it is better applied non-uniformly, to adults than to elderly.

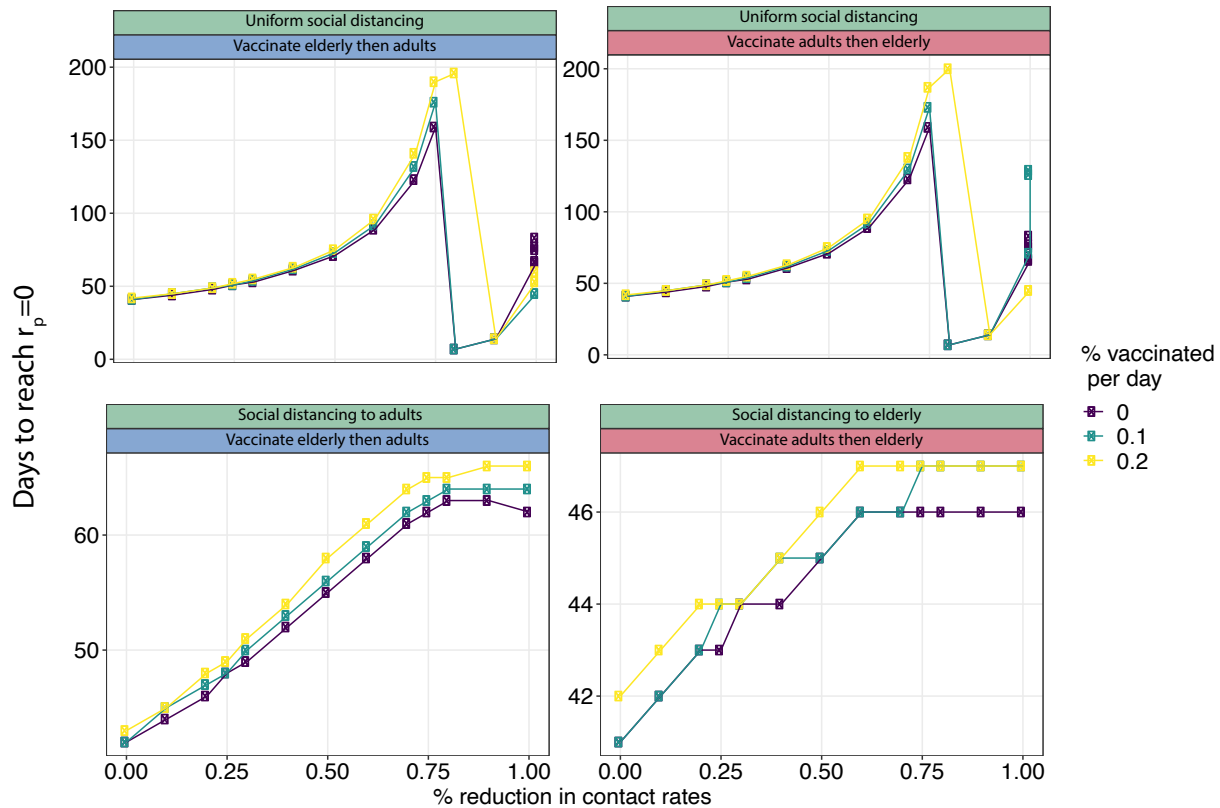


Figure 6: Time to obtain zero percent change in virus growth. The plot depicts r_p —the daily percent change in infected and asymptomatic individuals—as a function of increasing uniform (upper row) and targeted (lower row) social distancing (0: no social distancing; 1: no contacts). Square and line colors depict κ , the proportion of the population vaccinated per day. t_Z increases with social distancing. Two strategies are shown: Vaccinating all elderly (60+) and then all adults (20-59) (left column); and vaccinating adults and then elderly (right column). Notice how targeted social distancing dramatically decreases the days to achieve $r_p = 0$.

Methods

Ethics statement

All the data we use originates from publicly available resources, such as academic literature or online epidemiological sources. We do not use any clinical data that requires IRB.

Model structure

The model is a mass action model that reflects a situation in which the number of contacts is independent of the population size—a reasonable choice for directly-transmitted diseases [13]. It follows a population of N individuals, divided into nine age groups, depicted with the subscript j (Table S1) and is described in the following equations:

$$\frac{dS_j}{dt} = - \sum_l \beta_{jl}(I_l + A_l) \frac{S_j}{N_l} - \mu_j \frac{S_j}{L_j} \quad (3a)$$

$$\frac{dE_j}{dt} = \sum_l \beta_{jl}(I_l + A_l) \frac{S_j}{N_l} - \alpha E_j - \mu_j \frac{E_j}{L_j} \quad (3b)$$

$$\frac{dI_j}{dt} = (1 - m_j)\alpha E_j - \eta I_j \quad (3c)$$

$$\frac{dA_j}{dt} = m_j\alpha E_j - \gamma A_j - \mu_j \frac{A_j}{L_j} \quad (3d)$$

$$\frac{dR_j}{dt} = (1 - h_j)\eta I_j \quad (3e)$$

$$\frac{dU_j}{dt} = \gamma A_j - \mu_j \frac{U_j}{L_j} \quad (3f)$$

$$\frac{dH_j}{dt} = h_j\eta I_j \quad (3g)$$

$$\frac{dV_j}{dt} = \mu_j \quad (3h)$$

$$L_j = S_j + E_j + A_j + U_j \quad (3i)$$

Model states and parameters

Parameters for this kind of model are of two kinds. First, “biological” parameters, the variation of which is less related to country-specific demographics. These include, for example, recovery time (γ), the probability of developing an asymptomatic disease (m), incubation period (α), and age-dependent probability of hospitalization (h). We obtained these parameters from the literature (see below). Second, demographic “social” parameters that vary greatly between countries and include age structure and contact rates between age groups. We obtained age structure from <https://unctadstat.unctad.org/wds>. Contact rates were taken from Mossong et al. [14] because this is currently the most comprehensive empirical (not inferred, e.g. [15]) survey of contacts relevant for the transmission of diseases such as COVID19 (we used the Italian contact network for Israel as a one for Israel is not available but results were qualitatively consistent across countries, including Italy). Mossong et al. [14] defined physical contacts as those that included interactions such as a kiss or a handshake and nonphysical contacts as those involving being in close proximity for a

certain amount of time (e.g., a two-way conversation without skin-to-skin contact). Because SARS-COV-2 can also be transmitted via air droplets and aerosols, we included all physical contacts and those non-physical contacts that lasted for 15 minutes or more.

Individuals start at a susceptible state (S) and become infected upon an encounter with infectious individuals that are either symptomatic (I) or asymptomatic (A) at a rate specified in the infection matrix β_{lj} (we assume that asymptomatic and symptomatic people have the same infection rates). We calculated β_{lj} as the product of the infection probability q (equal across age) and contact rates between age groups j and l , given by the contact matrix C_{lj} :

$$\beta_{lj} = q \cdot C_{lj} \quad (4)$$

Infection due to an encounter with individuals from the same age group occurs when $l = j$. We halved the matrix diagonal to avoid counting the same interaction twice. We obtained C_{lj} for different countries from [14] using the R package `socialmixr`. The matrices describe the daily mean number of contacts that participants have with people at different age groups (Fig. S3). Next, we calculated the average rate of infection $\hat{\beta}$ by fitting an exponential model of the form $I(t) = e^{\hat{\beta}t}$ to Israeli case data (across ages) that describes the invasion of the virus to a completely susceptible population at the early stages of the disease (days 1-35, before interventions were forced; Fig. S4). This model gave a value of $\hat{\beta} = 0.24$ infections per day ($p < 0.001$, fit: $R^2 = 0.98$). However, $\hat{\beta}$ is an average across all the population. We therefore calculated the infection probability given an encounter between a susceptible and infected individuals as

$$q = \hat{\beta} / \langle C_{lj} \rangle . \quad (5)$$

Running the model without vaccination and starting with a single infected individual, we obtained the same initial disease dynamics and number of infected cases as observed in the data (Fig. S4).

Upon infection, the virus has a latency period of 6.4 days ($\alpha = 1/6.4$) [16], after which individuals become either asymptomatic with a probability m_j or develop symptoms with probability $1 - m_j$. The fraction of asymptomatic COVID19 infections was estimated at 30-40% [17]. In the absence of data on age-specific asymptomatic infections, we have set $m_j = 0.4$ for all ages. However, our model retains the flexibility to quantify the role of age-dependent asymptomatic probabilities in COVID19 epidemiology (m_j) because a previous study on corona viruses (not including SARS-COV-2) found that children tend to be less symptomatic than adults [18].

Asymptomatic individuals stop infecting (U) within 7 days ($\gamma = 1/7$) – an estimate from [19] that lies between that of [20] (mean 5 days) and that of [21] (mean 11 days). Results were qualitatively the same when we used the estimate by Davies et al [20], also used in [10]. We assume that symptomatic individuals are identified and removed to quarantine (R) within 1.5 days ($\eta = 1/(1.5)$); results were qualitatively the same when we used $\eta = 1$ or $\eta = 1/2$. Depending on age, with probability h_j individuals can develop severe symptoms and be hospitalized (H). We calculated h_j using data from the Israel Ministry of Health as the fraction of hospitalized cases out of those that showed symptoms. This probability is not expected to vary greatly between countries as age-dependent hospitalization has a strong biological rather than social component in countries which are culturally similar. Effectively, individuals in states V , U , R and H cannot further infect. Separating between R and U is useful for scenarios in which quarantine should be considered separately than asymptomatic recovery (e.g., for economic reasons because some quarantined individuals

cannot work).

Interventions

Vaccination We administer vaccines to people in states S , E , A , U , as they have not shown symptoms and are therefore considered susceptible from a public health perspective. We assume a non-leaky vaccine (prevents transmission) and that the vaccine affects all individuals in the same way. Vaccines are deployed from the beginning of the simulation at a constant rate κ vaccines per day, which we measure as the percentage of population that a government can vaccinate a day. For example, in Israel (population about 8.7 million), vaccinating 0.2% of the population every day translates into deployment of about 17400 vaccines daily and over 1.5 million vaccines in the course of 90 days.

The number of daily vaccines is divided equally across the target age groups. For example, if the strategy is to vaccinate adults 60+, then each of the age groups 60-69, 70-79 and 80+ will get $\mu_j = \kappa/3$ vaccines. The μ_j vaccines are deployed to states S_j , E_j , A_j and U_j according to their relative proportions in the group (see last terms in equations 3a, 3b, 3d and 3f and equation 3i). The model allows for dynamic prioritization by selecting an order of preferred target groups. For example, a strategy of vaccinating 60+ and then 20-59 will first deploy vaccines to the age groups 60-69, 70-99, and 80+ as described above. Then, when there are no individuals left to vaccinate, the model will switch to vaccinating individuals 20-59.

Social distancing Social distancing is the act of reducing contacts. Hence, we define $\beta_{lj}^S = (1 - x_{lj})\beta_{lj}$, where elements of x_{lj} range between 0 (no social distancing) and 1 (no contacts whatsoever), and act to reduce contacts within and between groups. x_{lj} is the quantity depicted on the x-axis of figures (e.g., Fig. 4). We note that the multiplication $x_{lj}\beta_{lj}$ is an element-by-element multiplication rather than a matrix multiplication and that intervention is symmetric. For example, $x_{1,1} = 0.4$ will reduce contacts between juveniles within the age group 0-9 to 60% of the non-intervention level and $x_{3,1} = x_{1,3} = 0.9$ is a strong social distancing intervention reducing contacts between age groups 0-9 and 20-29 to 10% of their non-intervention level.

Code availability

All analyses were performed in R and the code is fully available in https://github.com/Ecological-Complexity-Lab/COVID19_vaccine_model.

Discussion

We used an age-structured model to explore the joint effects of vaccination and social-distancing interventions on COVID19 disease dynamics. While social distancing delays infections that result in hospitalizations, vaccination can reduce the total number of hospitalizations. Hence, a combination of these two strategies provides greater benefits than their isolated deployment. Despite the synergism between these intervention methods, when social distancing is applied uniformly it overrides the need for vaccinations if applied too strongly (beyond a threshold), leading to a decrease in vaccine efficiency. Social distancing targeted only at adults removes this threshold because it prevents infection of the elderly from adults while protecting elderly via vaccination. Hence, both interventions are effectively working in parallel on different populations.

Nevertheless, vaccination has little effect on the time it takes to eliminate the disease. This is because vaccine is deployed during the pandemic, while non-vaccinated individuals continuously get infected. By contrast, social distancing delays the time to disease elimination by preventing infections. Therefore, social distancing is a strategy to “flatten the curve” but, as we show here, the way that it is applied and combined with vaccinations is important. Under uniform social distancing, in which a greater portion of the population is not infected (compared to targeted social distancing), the time it takes to mitigate the disease is longer than under a targeted social distancing scenario. Taken together, our results clearly show that vaccinating elderly in the ages of 60+ while applying social distancing to adults (20-59) is an optimal strategy and that this is driven by the higher probability of severe infections in elderly. These findings are in line with another study of vaccine prioritization [10].

Modeling is instrumental to informing policy makers and the public about possible scenarios of disease progression and the potential efficacy of different intervention methods [12, 22–24]. It is also true, however, that even now we have limited knowledge on the biology and epidemiology of the SARS-COV-2 virus, hampering our ability to correctly parameterize models and that parameter values vary between human populations and countries. Inaccurate parameterization and ignoring model assumptions (e.g., geographical heterogeneity) could potentially lead to erroneous conclusions [25]. Our model assumes homogeneous mixing in space and reflects an average population – for example, it does not include household, school, or work dynamics, which are relevant when investigating epidemic infections via contacts.

Nevertheless, when interpreted within the known limitations, this study provides valuable insights into the joint effect of vaccination and social distancing and the mechanisms underlying their interplay. It also provides initial guidelines for policy makers. For example, we find that the same level of overall efficiency in reducing hospitalizations can be obtained via different combinations of social distancing, vaccine prioritization and vaccine deployment rates, providing policy makers with a range of possibilities. Moreover, our model can be readily used and easily modified to generate and test a range of hypotheses and strategies for vaccination. For example, policy-makers can examine strategies that reduce deaths or those that prioritize vaccines to adults to avoid economic inactivity. Such strategies and others can be tested by modifying the effectiveness measure F_X where X may be any combination of $S, E, I, A, U, R, H,$ and V . In addition, we did not include children in our targeted interventions because vaccine is not available for them (yet), and to reduce the complexity of the experimental design. Future studies can test the effect of social distancing and/or vaccination targeted at children. Finally, it will also be important to include information on proportion of people that refuse to take a vaccine.

This study deals with an ethical question: Who should be vaccinated first? We do not presume to answer this question, to which some guidelines have been laid out [8, 9]. We do, however, advocate for a mechanistic understanding of the factors that affect vaccination success and how to combine intervention strategies in a way that will align with those ethical guidelines. Our study provides one way towards these goals.

Acknowledgments

We thank Profs. Yoav Tsori and Roni Granek for comments on a previous version of the model. This research was supported by the Ministry of Science & Technology, Israel (grant no. 3-16893).

References

1. Lee, B. Y. *et al.* A computer simulation of vaccine prioritization, allocation, and rationing during the 2009 H1N1 influenza pandemic. *Vaccine* **28**, 4875–4879. doi:[10.1016/j.vaccine.2010.05.002](https://doi.org/10.1016/j.vaccine.2010.05.002) (2010).
2. Barrot, J.-N., Grassi, B. & Sauvagnat, J. *Sectoral Effects of Social Distancing* 2020.
3. Venkatesh, A. & Edirappuli, S. Social distancing in covid-19: what are the mental health implications? *BMJ* **369**, m1379. doi:[10.1136/bmj.m1379](https://doi.org/10.1136/bmj.m1379) (2020).
4. Balicer, R. D., Huerta, M., Davidovitch, N. & Grotto, I. Cost-benefit of stockpiling drugs for influenza pandemic. *Emerg. Infect. Dis.* **11**, 1280–1282. doi:[10.3201/eid1108.041156](https://doi.org/10.3201/eid1108.041156) (2005).
5. Khamsi, R. If a coronavirus vaccine arrives, can the world make enough. *Nature* **580**, 578. doi:[10.1038/d41586-020-01063-8](https://doi.org/10.1038/d41586-020-01063-8) (2020).
6. Matrajt, L., Eaton, J., Leung, T. & Brown, E. R. Vaccine optimization for COVID-19, who to vaccinate first? *medRxiv*. doi:[10.1101/2020.08.14.20175257](https://doi.org/10.1101/2020.08.14.20175257) (2020).
7. Gallagher, M. E. *et al.* Considering indirect benefits is critical when evaluating SARS-CoV-2 vaccine candidates. *medRxiv*. doi:[10.1101/2020.08.07.20170456](https://doi.org/10.1101/2020.08.07.20170456) (2020).
8. Cohen, J. The line is forming for a COVID-19 vaccine. Who should be at the front. *Science* **369**, 15–16 (2020).
9. Emanuel, E. J. *et al.* An ethical framework for global vaccine allocation. *Science* **369**, 1309–1312. doi:[10.1126/science.abe2803](https://doi.org/10.1126/science.abe2803) (2020).
10. Bubar, K. M. *et al.* Model-informed COVID-19 vaccine prioritization strategies by age and serostatus. *medRxiv*. doi:[10.1101/2020.09.08.20190629](https://doi.org/10.1101/2020.09.08.20190629) (2020).
11. Jentsch, P., Anand, M. & Bauch, C. T. *Prioritising COVID-19 vaccination in changing social and epidemiological landscapes* 2020.
12. Ferguson, N *et al.* *Impact of non-pharmaceutical interventions (NPIs) to reduce COVID-19 mortality and healthcare demand* tech. rep. (Imperial College, 2020). doi:[10.25561/77482](https://doi.org/10.25561/77482).
13. Keeling, M. J. & Rohani, P. *Modeling infectious diseases in humans and animals* (eds Keeling, M. J. & Rohani, P.) (Princeton University Press, Princetone, New Jersey, 2008).
14. Mossong, J. *et al.* Social contacts and mixing patterns relevant to the spread of infectious diseases. *PLoS Med.* **5**, e74. doi:[10.1371/journal.pmed.0050074](https://doi.org/10.1371/journal.pmed.0050074) (2008).
15. Prem, K., Cook, A. R. & Jit, M. Projecting social contact matrices in 152 countries using contact surveys and demographic data. *PLoS Comput. Biol.* **13**, e1005697. doi:[10.1371/journal.pcbi.1005697](https://doi.org/10.1371/journal.pcbi.1005697) (2017).
16. Backer, J. A., Klinkenberg, D. & Wallinga, J. Incubation period of 2019 novel coronavirus (2019-nCoV) infections among travellers from Wuhan, China, 20-28 January 2020. *Euro Surveill.* **25**. doi:[10.2807/1560-7917.ES.2020.25.5.2000062](https://doi.org/10.2807/1560-7917.ES.2020.25.5.2000062) (2020).
17. Lavezzo, E. *et al.* Suppression of a SARS-CoV-2 outbreak in the Italian municipality of Vo'. *Nature* **584**, 425–429. doi:[10.1038/s41586-020-2488-1](https://doi.org/10.1038/s41586-020-2488-1) (2020).
18. Galanti, M *et al.* Rates of asymptomatic respiratory virus infection across age groups. *Epidemiol. Infect.* **147**, e176. doi:[10.1017/S0950268819000505](https://doi.org/10.1017/S0950268819000505) (2019).

19. Cheng, H.-Y. *et al.* Contact Tracing Assessment of COVID-19 Transmission Dynamics in Taiwan and Risk at Different Exposure Periods Before and After Symptom Onset. *JAMA Intern. Med.* **180**, 1156–1163. doi:[10.1001/jamainternmed.2020.2020](https://doi.org/10.1001/jamainternmed.2020.2020) (2020).
20. Davies, N. G. *et al.* Age-dependent effects in the transmission and control of COVID-19 epidemics. *Nat. Med.* **26**, 1205–1211. doi:[10.1038/s41591-020-0962-9](https://doi.org/10.1038/s41591-020-0962-9) (2020).
21. Zou, L. *et al.* SARS-CoV-2 Viral Load in Upper Respiratory Specimens of Infected Patients. *N. Engl. J. Med.* **382**, 1177–1179. doi:[10.1056/NEJMc2001737](https://doi.org/10.1056/NEJMc2001737) (2020).
22. Colbourn, T. COVID-19: extending or relaxing distancing control measures. *Lancet Public Health* **5**, e236–e237. doi:[10.1016/S2468-2667\(20\)30072-4](https://doi.org/10.1016/S2468-2667(20)30072-4) (2020).
23. Karin, O. *et al.* Adaptive cyclic exit strategies from lockdown to suppress COVID-19 and allow economic activity. *medRxiv*. doi:[10.1101/2020.04.04.20053579](https://doi.org/10.1101/2020.04.04.20053579) (2020).
24. Prem, K. *et al.* The effect of control strategies to reduce social mixing on outcomes of the COVID-19 epidemic in Wuhan, China: a modelling study. *Lancet Public Health* **5**, e261–e270. doi:[10.1016/S2468-2667\(20\)30073-6](https://doi.org/10.1016/S2468-2667(20)30073-6) (2020).
25. Holmdahl, I. & Buckee, C. *Wrong but Useful — What Covid-19 Epidemiologic Models Can and Cannot Tell Us* 2020. doi:[10.1056/nejmp2016822](https://doi.org/10.1056/nejmp2016822).

Supplementary Information

S1 Methods

Table S1: Population structure of Israel and relevant parameters. j is the ID of the age group; Proportion is the proportion of the age group in the Israeli population; h_j is the probability of hospitalization taken from <https://datadashboard.health.gov.il/COVID-19/general>. This probability is not expected vary greatly between countries as age-dependent hospitalization has a strong biological rather than social component in countries which are culturally similar.

i	Age	Proportion	h_j
1	0-9	0.20	0.05
2	10-19	0.16	0.04
3	20-29	0.14	0.10
4	30-39	0.13	0.12
5	40-49	0.12	0.17
6	50-59	0.09	0.24
7	60-69	0.08	0.34
8	70-79	0.05	0.52
9	80+	0.03	0.73

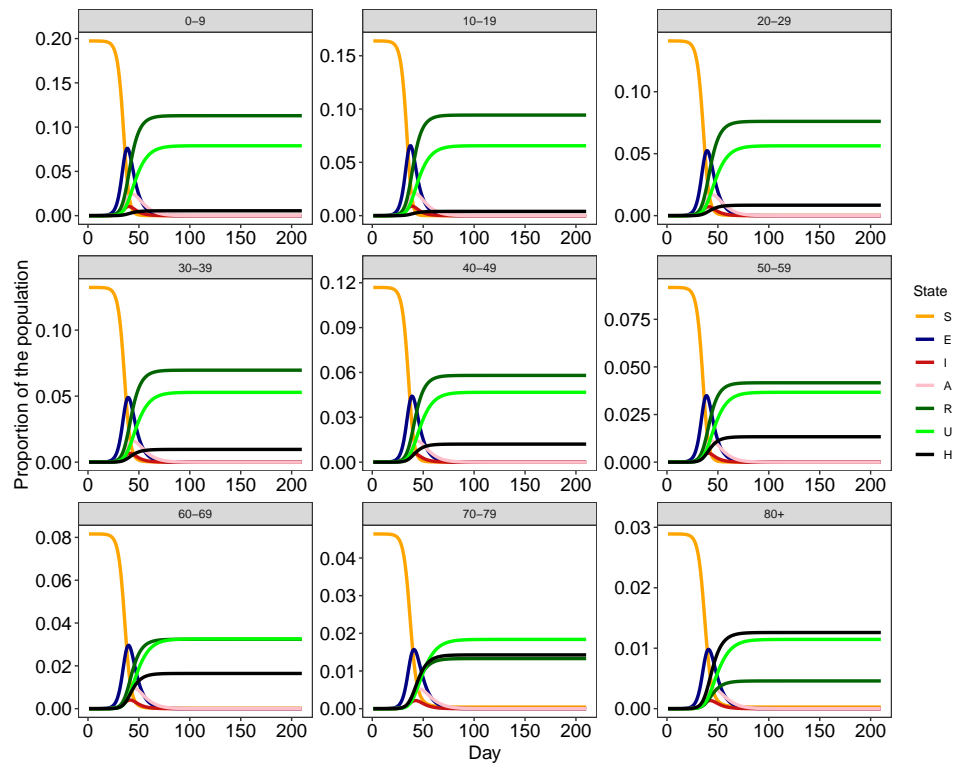


Figure S1: Epidemiological curves without vaccine. Epidemiological curves for the baseline model, with no vaccination or social distancing. *S*: susceptible; *E*: exposed; *I*: infectious and symptomatic; *A*: infectious and asymptomatic; *R*: removed to quarantine and then recovered naturally, and immune; *U*: recovered naturally, and immune; *H*: hospitalized.

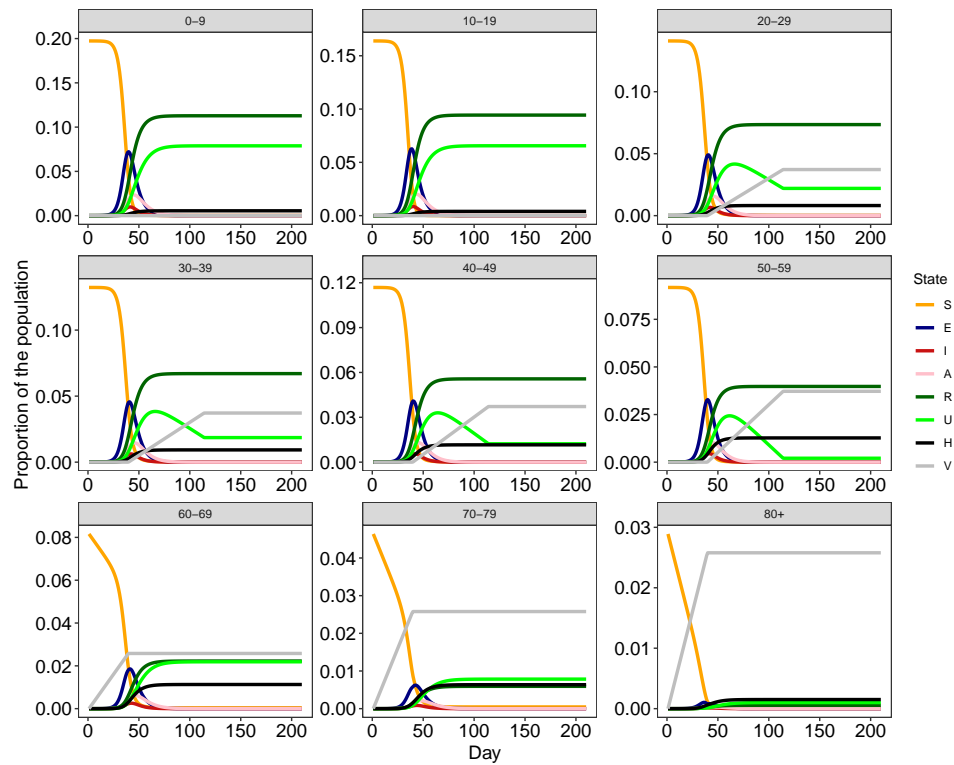


Figure S2: Epidemiological curves with vaccine. Epidemiological curves with vaccination ($\kappa = 0.2$) and no social distancing. *S*: susceptible; *E*: exposed; *I*: infectious and symptomatic; *A*: infectious and asymptomatic; *R*: removed to quarantine and then recovered naturally, and immune; *U*: recovered naturally, and immune; *H*: hospitalized; *V*: vaccinated.

It is made available under a [CC-BY-NC-ND 4.0 International license](https://creativecommons.org/licenses/by-nc-nd/4.0/).

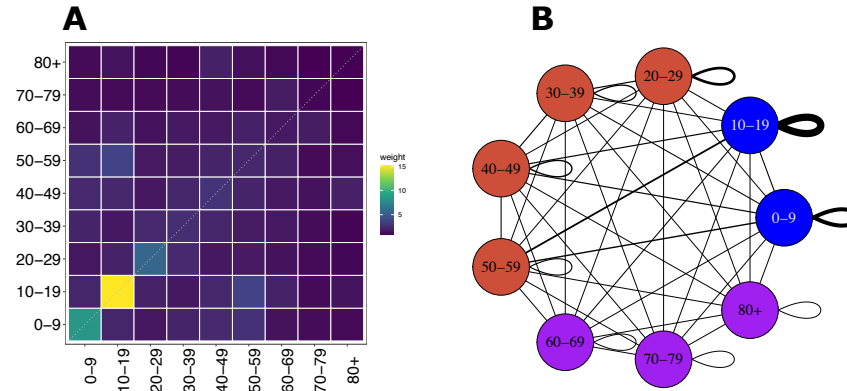


Figure S3: An example of an age-dependent contact rates. (A) Contact matrix for Italy calculated from data collected by [14]. Matrix cells depict the mean number of daily contacts between people in different age groups. Diagonal cells depict contacts between individuals from the same age group. (B) The same data as in (A), represented as a network of contacts. Edge widths depict contact rates.

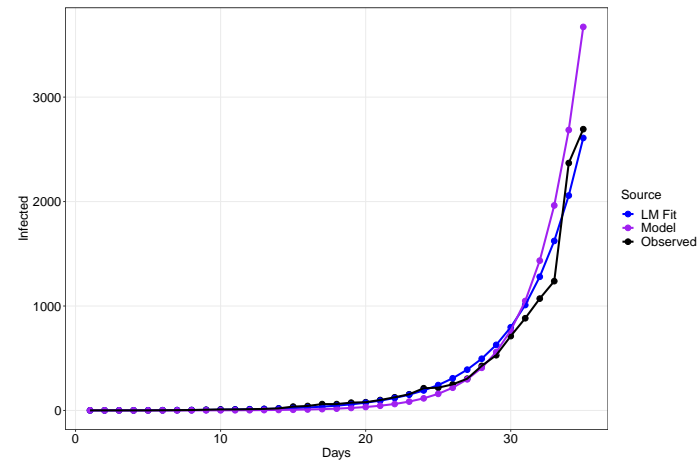


Figure S4: Fitting curve for Israeli case data. We calculated the average rate of infection $\hat{\beta}$ by fitting an exponential model of the form $I(t) = e^{\hat{\beta}t}$ (blue) to observed case data across ages at the early stages of the disease (days 1-35, before the lock-down; black curve). The exponential fit gave a value of $\hat{\beta} = 0.24$ ($p < 0.001$, $R^2 = 0.98$). Our epidemiological model (Fig. 1 in the main text) produced similar curve (purple), indicating that our choice of parameters was reasonable. The source of the observed data is <https://github.com/CSSEGISandData/COVID-19>.

S2 Results

S2.1 Social distancing and vaccination

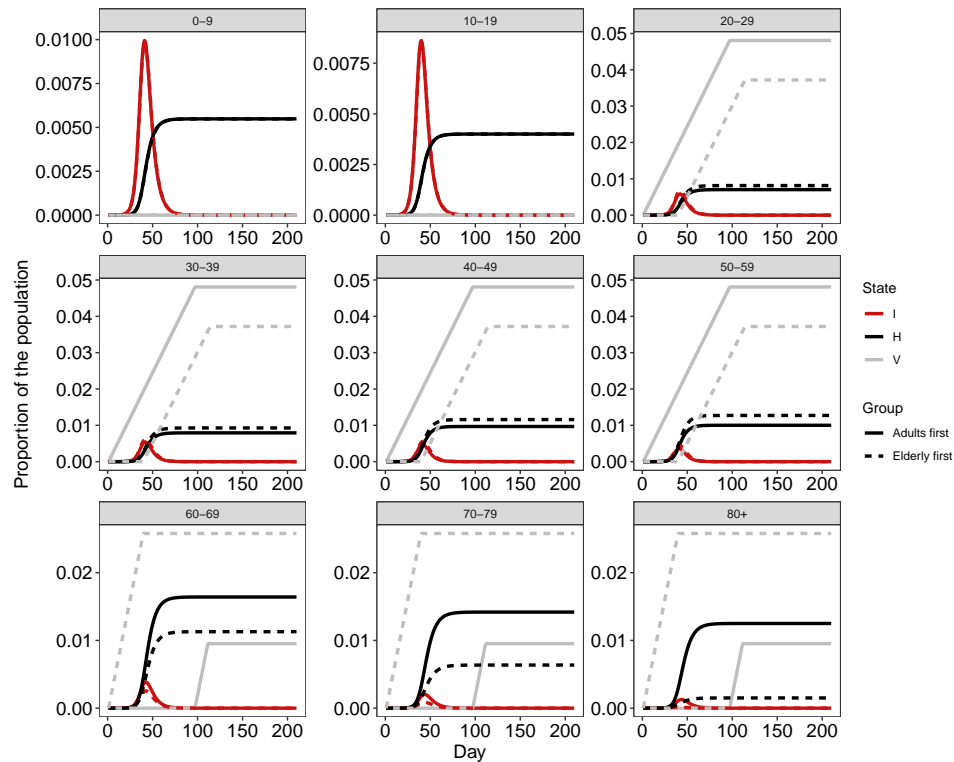


Figure S5: Comparison of dynamics between two prioritization strategies. Dashed and solid lines depict two strategies, respectively: (i) vaccinating all elderly (60+) and then all adults (20-59) and (ii) vaccinating all adults and then all elderly. This example is for $\kappa = 0.2$ (0.2% of the population is vaccinated per day) and there is no social distancing. In the first strategy, around 40 days there are no more elderly to vaccinate and the model shifts to vaccinating adults (gray solid line). In the second strategy the number of adults in the population is large and the switch to vaccinating elderly occurs after about 90 days. It is clear that most of the reduction in hospitalizations is obtained when the elderly are prioritized. I : infectious and symptomatic (red); H : hospitalized (black); V : vaccinated (gray).

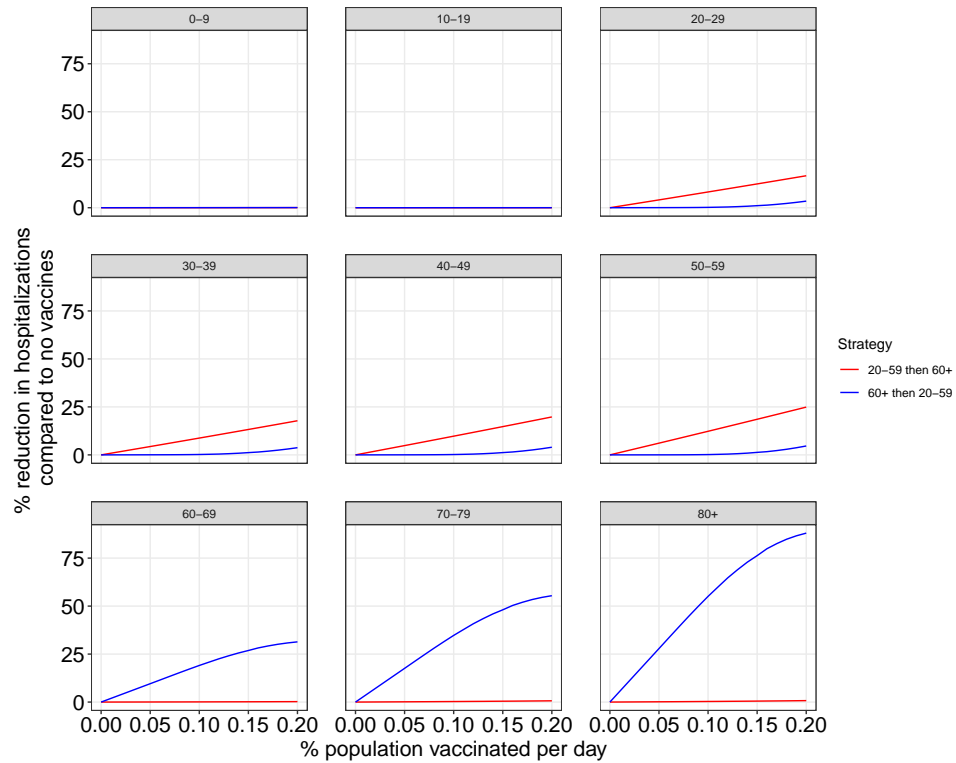


Figure S6: Comparison between prioritization strategies with no social distancing per age group. The plot depicts the F_H^j (y-axis) as a function of increasing vaccination rates (κ), measured as the proportion of the population vaccinated per day (e.g., $\kappa = 0.2$ translates to deployment of 16,000 vaccines per day in a population of 8 million people). Each panel shows the effect of vaccination on a particular age group (F_H^j). It is clear that vaccinating a certain group has a larger effect on that group (compare for example the red line to the blue line in the 50-59 age group).

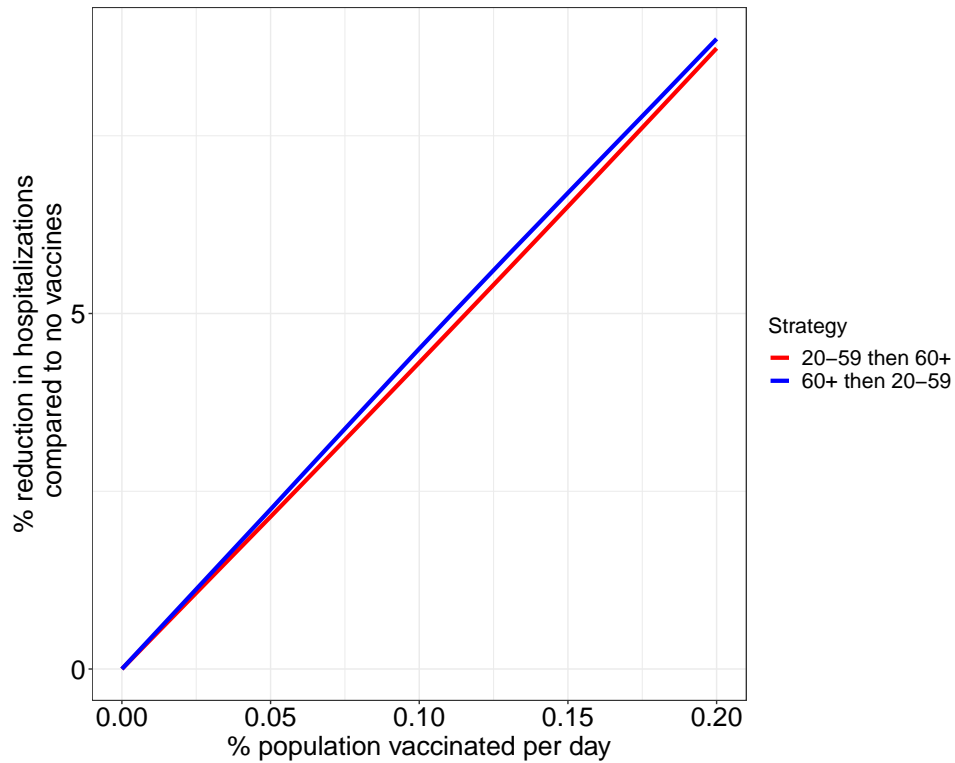


Figure S7: Comparison between prioritization strategies with no social distancing and age-uniform hospitalization probabilities. The plot depicts the F_H^{tot} (y-axis) as a function of increasing vaccination rates (κ), measured as the proportion of the population vaccinated per day (e.g., $\kappa = 0.2$ translates to deployment of 16,000 vaccines per day in a population of 8 million people. Vaccinating elderly (60+) and then adults (20-59)—depicted in the blue line—is more effective than vaccinating adults and then elderly (red line). Probability of hospitalization equals to 10% across all age 9 groups.

S2.2 Growth rate measures

S2.2.1 Percent change in I+A

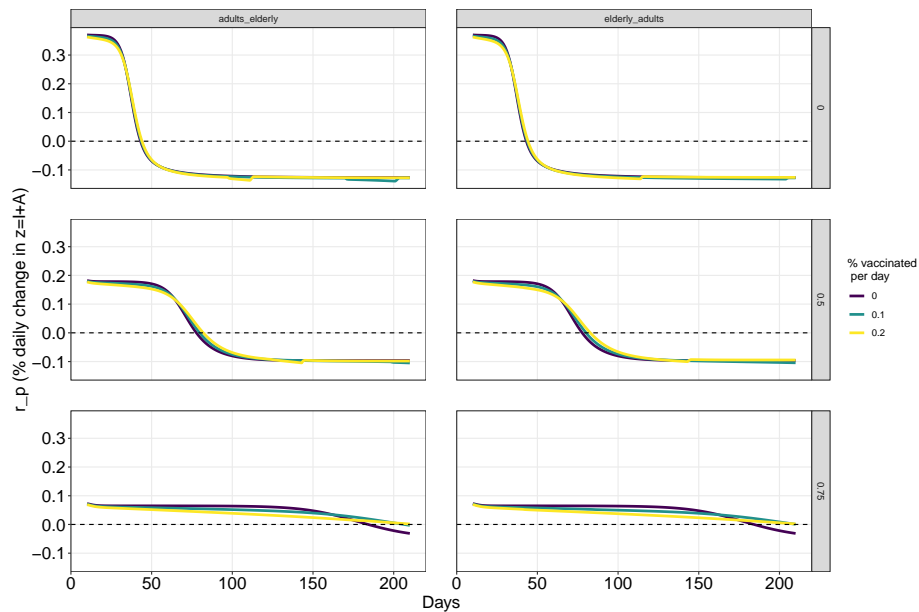


Figure S8: Daily change in r_p . The plot depicts r_p (y-axis)—the daily percent change in infected and asymptomatic individuals—as a function of time. Social distancing is applied uniformly to all the population. Three values of % reduction in contacts are shown in rows.

S2.2.2 Growth rate lower than 0

We calculate the growth rate of infected and asymptomatic individuals from equations 3c and 3d as $r = dI_j/dt + dA_j/dt = \alpha E_j - \eta I_j - \gamma A_j - \mu A_j/L_j$, and we look for the time in which $r \leq 0$. The units of r are individuals per day. We find a general pattern in which growth rate peaks (many new cases) and decreases to 0, which corresponds to the time in which the pool of I and A compartments is more or less equal to that of the exposed (E). After that point, the number of new infections (E) is much lower than the number of individuals already sick ($I + A$), causing a negative growth. Afterwards, as individuals move from the I and A compartments growth stabilizes on 0. As is the case for r_p , social distancing and not vaccination is the major factor affecting elimination, which is slowed down by stronger social distancing.

It is made available under a [CC-BY-NC-ND 4.0 International license](https://creativecommons.org/licenses/by-nc-nd/4.0/).

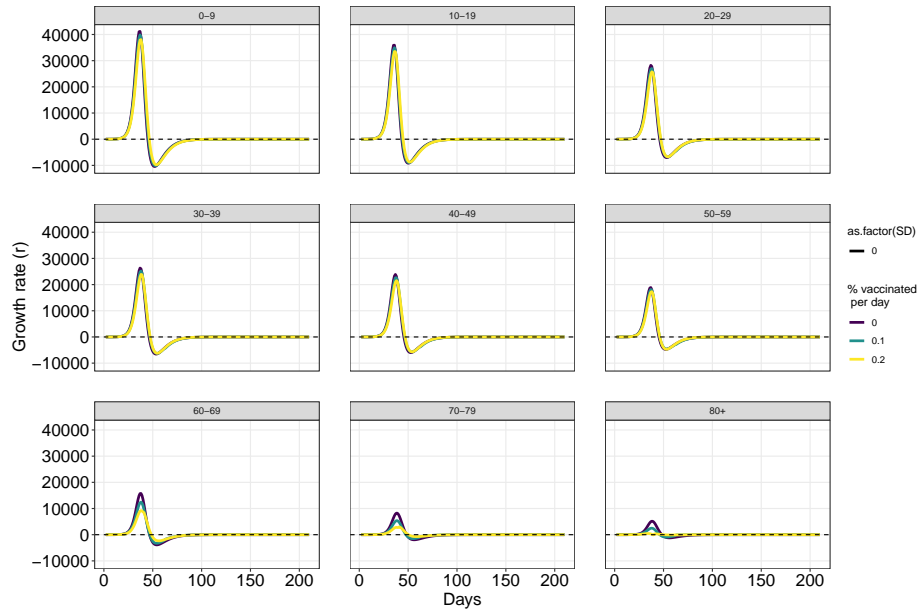


Figure S9: Growth rate with no social distancing. The plot depicts daily values of growth rate r , defined as $r = dI_j/dt + dA_j/dt$ in units of individuals per day. The plot is for a strategy in which elderly (60+) are vaccinated first and then all adults (20-59). Line colors depict κ , the proportion of the population vaccinated per day.

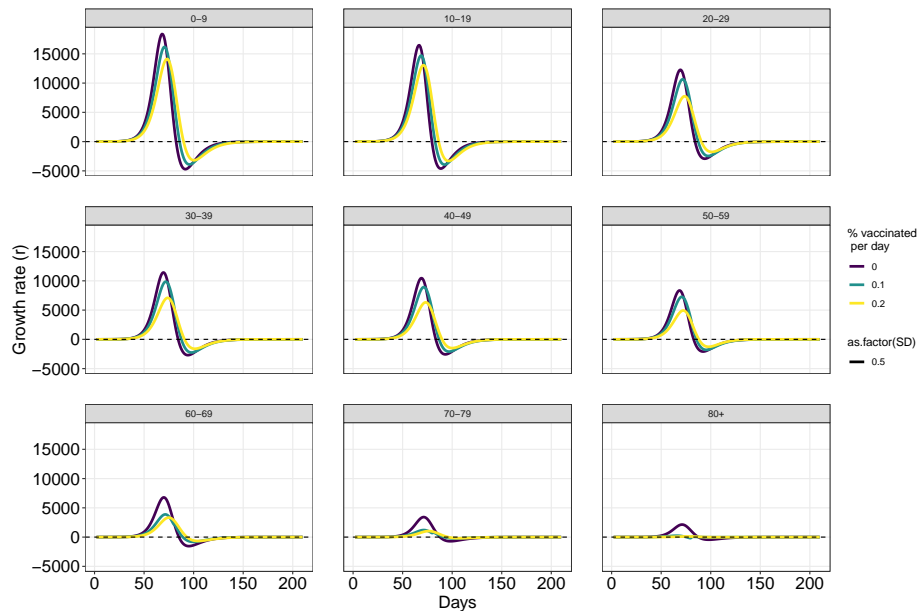


Figure S10: Growth rate with uniform social distancing of 50%. The plot depicts daily values of growth rate r , defined as $r = dI_j/dt + dA_j/dt$ in units of individuals per day. The plot is for a strategy in which elderly (60+) are vaccinated first and then all adults (20-59). Line colors depict κ , the proportion of the population vaccinated per day.

It is made available under a [CC-BY-NC-ND 4.0 International license](https://creativecommons.org/licenses/by-nc-nd/4.0/) .

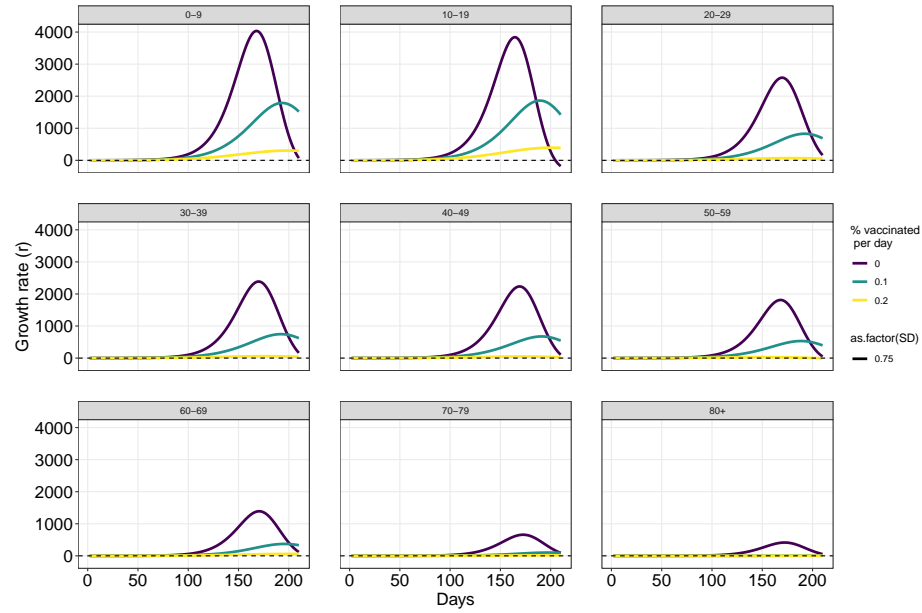


Figure S11: Growth rate with uniform social distancing of 75%. The plot depicts daily values of growth rate r , defined as $r = dI_j/dt + dA_j/dt$ in units of individuals per day. The plot is for a strategy in which elderly (60+) are vaccinated first and then all adults (20-59). Line colors depict κ , the proportion of the population vaccinated per day.

S3 Other countries

S3.1 Belgium

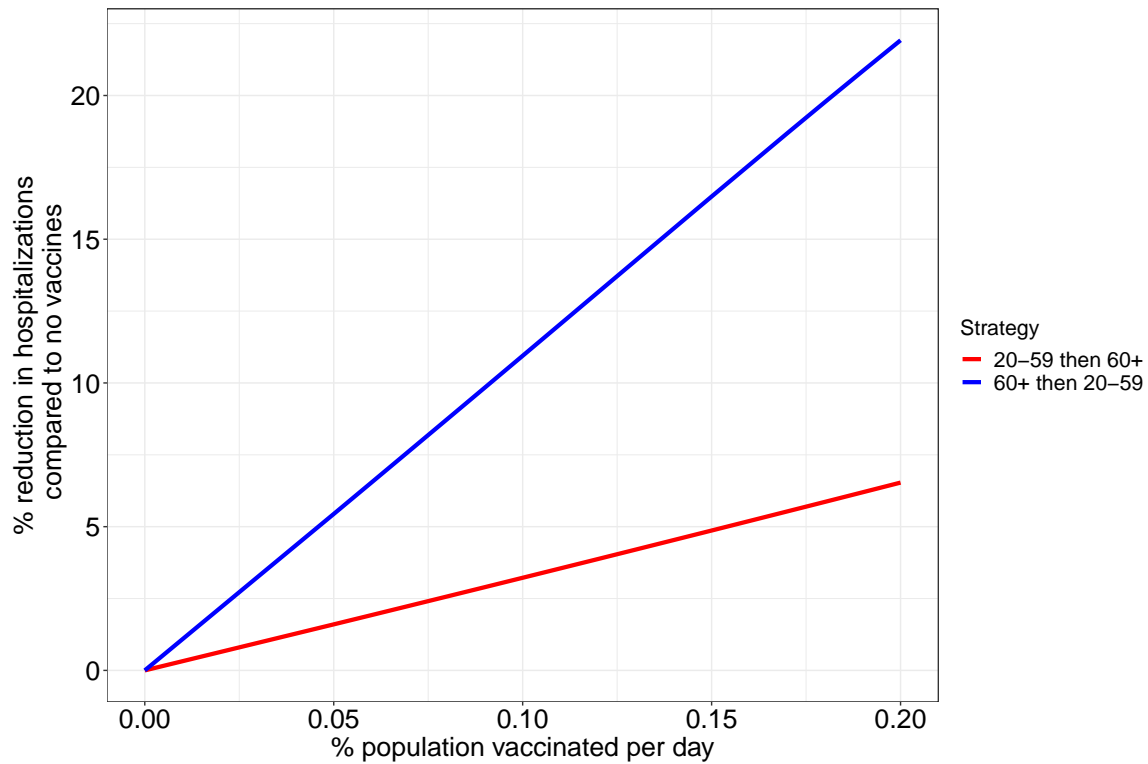


Figure S12: Comparison between prioritization strategies with no social distancing. The plot depicts the F_H^{tot} (y-axis) as a function of increasing vaccination rates (κ), measured as the proportion of the population vaccinated per day. Vaccinating elderly (60+) and then adults (20-59)—depicted in the blue line—is more effective than vaccinating adults and then elderly (red line).

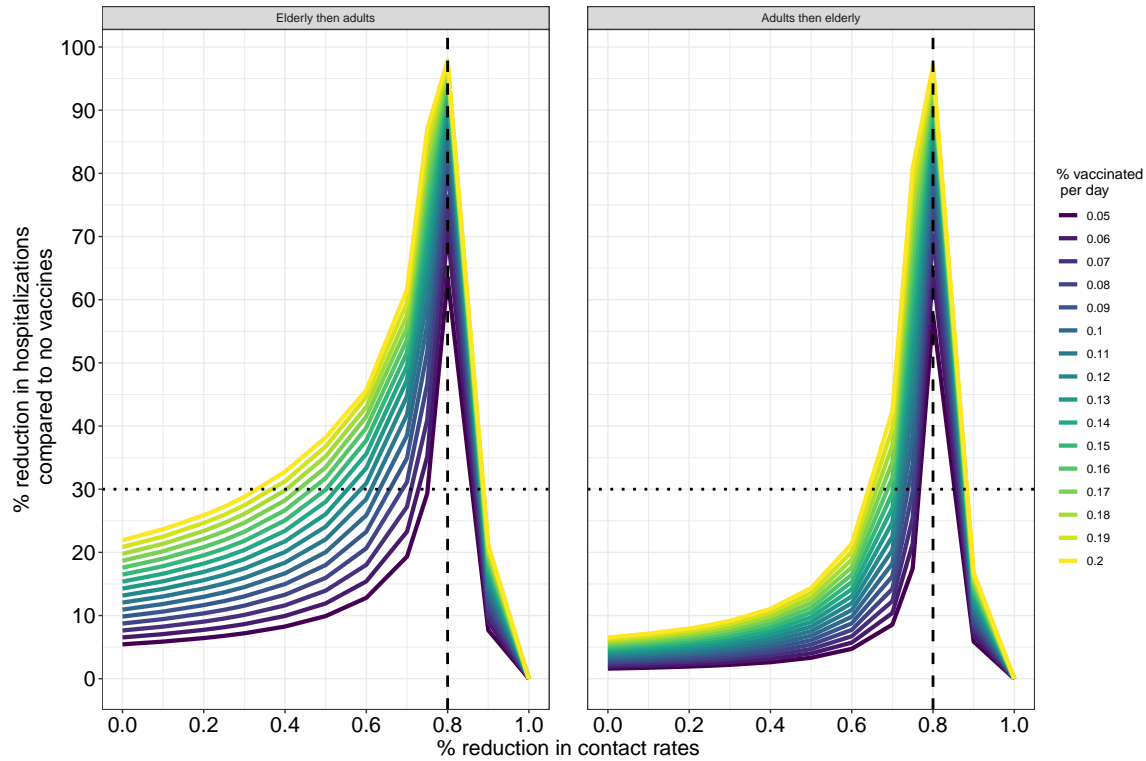


Figure S13: Comparison between prioritization strategies with uniform social distancing. The plot depicts the F_H^{tot} (y-axis) as a function of increasing social distancing (0: no social distancing; 1: no contacts). Line colors depict κ , the proportion of the population vaccinated per day. Two strategies are shown: Vaccinating all elderly (60+) and then all adults (20-59) (left panel); and vaccinating adults and then elderly (right panel). In both strategies there is a threshold of reduction in contacts (dashed vertical line) above which vaccination is no longer effective. Horizontal dotted line provides an example of how the same level of reduction in hospitalizations (here, $F_H^{tot} = 0.3$) can be achieved using different combinations of social distancing, vaccine prioritization and vaccine deployment rates.

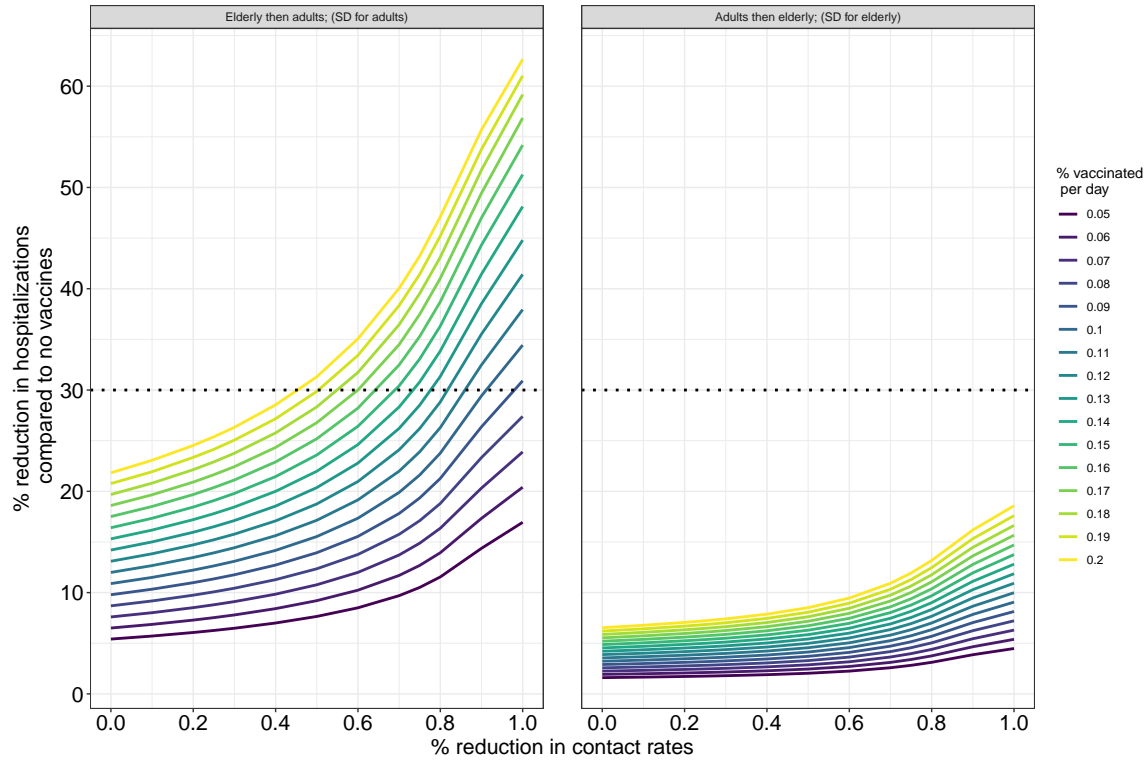


Figure S14: Comparison between prioritization strategies with targeted social distancing. The plot depicts the F_H^{tot} (y-axis) as a function of increasing social distancing (0: no social distancing; 1: no contacts). Line colors depict κ , the proportion of the population vaccinated per day. Two strategies are shown: Vaccinating all elderly (60+) and then all adults (20-59), while applying social distancing only in the adult group (left panel); and vaccinating adults and then elderly, while applying social distancing only in the elderly group (right panel). Horizontal dotted line at $F_H^{tot} = 0.3$ is the same as in Fig. 4 and shows that vaccines has very little in reducing hospitalization when prioritized to adults.

S3.2 Italy

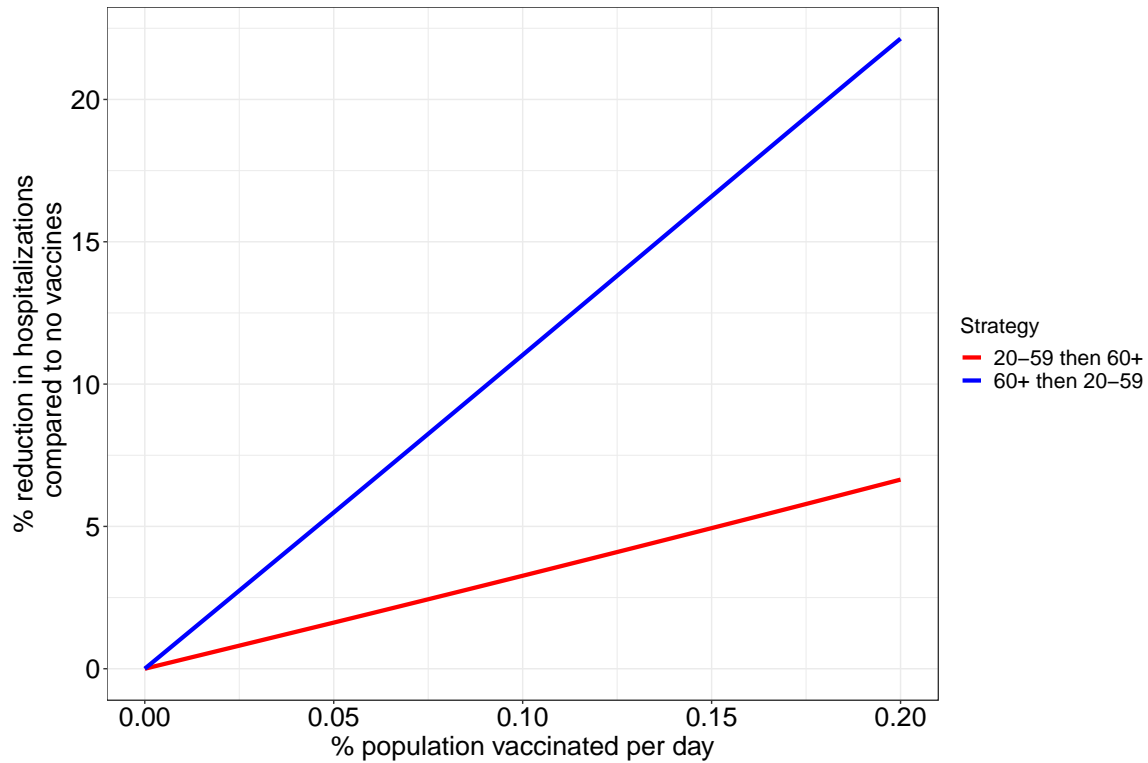


Figure S15: Comparison between prioritization strategies with no social distancing. The plot depicts the F_H^{tot} (y-axis) as a function of increasing vaccination rates (κ), measured as the proportion of the population vaccinated per day. Vaccinating elderly (60+) and then adults (20-59)—depicted in the blue line—is more effective than vaccinating adults and then elderly (red line).

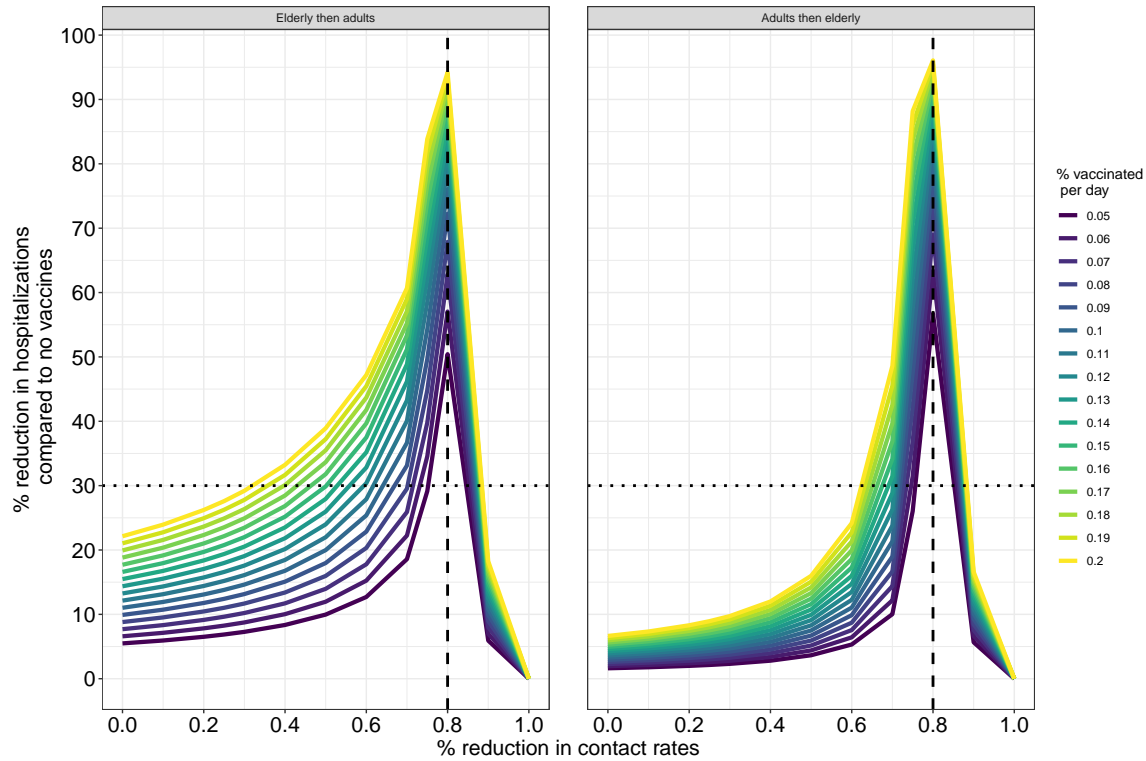


Figure S16: Comparison between prioritization strategies with uniform social distancing. The plot depicts the F_H^{tot} (y-axis) as a function of increasing social distancing (0: no social distancing; 1: no contacts). Line colors depict κ , the proportion of the population vaccinated per day. Two strategies are shown: Vaccinating all elderly (60+) and then all adults (20-59) (left panel); and vaccinating adults and then elderly (right panel). In both strategies there is a threshold of reduction in contacts (dashed vertical line) above which vaccination is no longer effective. Horizontal dotted line provides an example of how the same level of reduction in hospitalizations (here, $F_H^{tot} = 0.3$) can be achieved using different combinations of social distancing, vaccine prioritization and vaccine deployment rates.

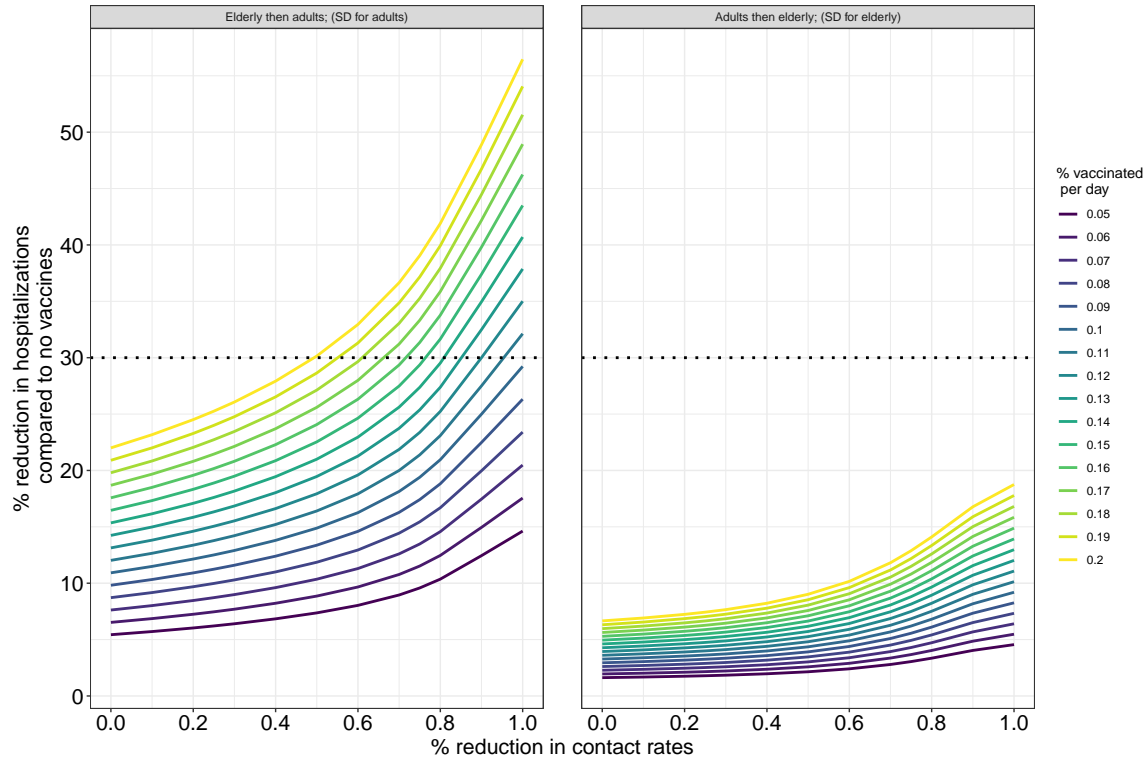


Figure S17: Comparison between prioritization strategies with targeted social distancing. The plot depicts the F_H^{tot} (y-axis) as a function of increasing social distancing (0: no social distancing; 1: no contacts). Line colors depict κ , the proportion of the population vaccinated per day. Two strategies are shown: Vaccinating all elderly (60+) and then all adults (20-59), while applying social distancing only in the adult group (left panel); and vaccinating adults and then elderly, while applying social distancing only in the elderly group (right panel). Horizontal dotted line at $F_H^{tot} = 0.3$ is the same as in Fig. 4 and shows that vaccines has very little in reducing hospitalization when prioritized to adults.

S3.3 Finland

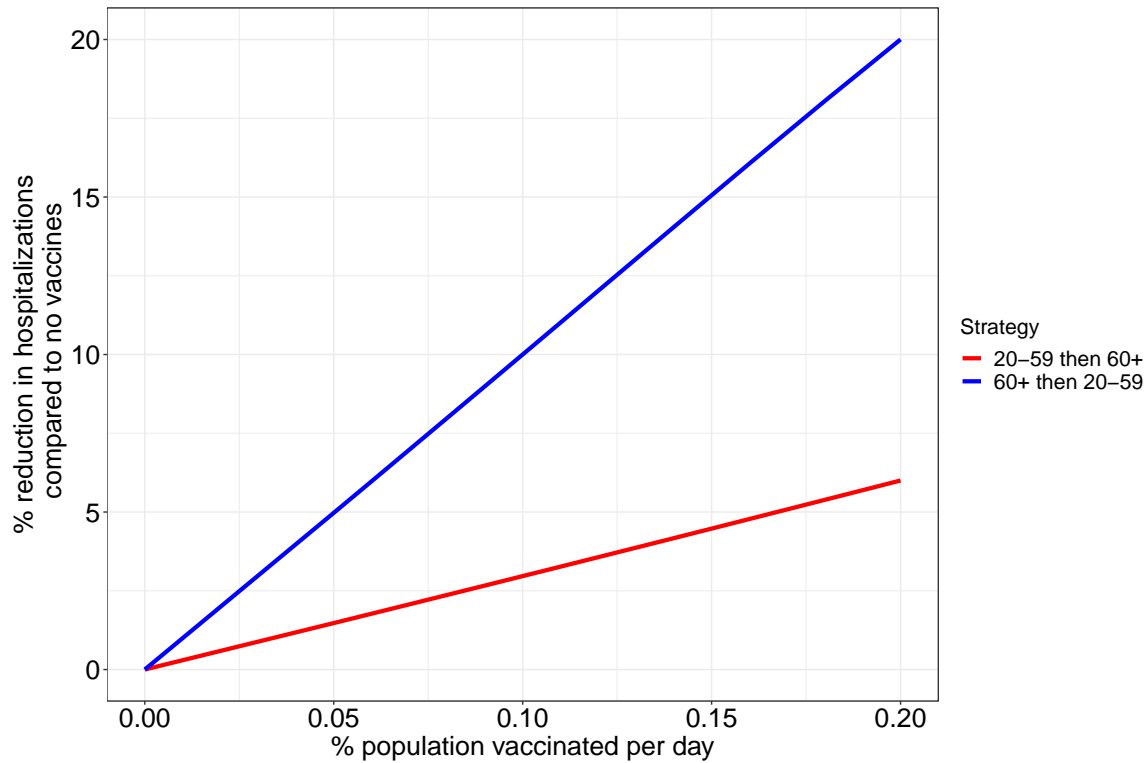


Figure S18: Comparison between prioritization strategies with no social distancing. The plot depicts the F_H^{tot} (y-axis) as a function of increasing vaccination rates (κ), measured as the proportion of the population vaccinated per day. Vaccinating elderly (60+) and then adults (20-59)—depicted in the blue line—is more effective than vaccinating adults and then elderly (red line).

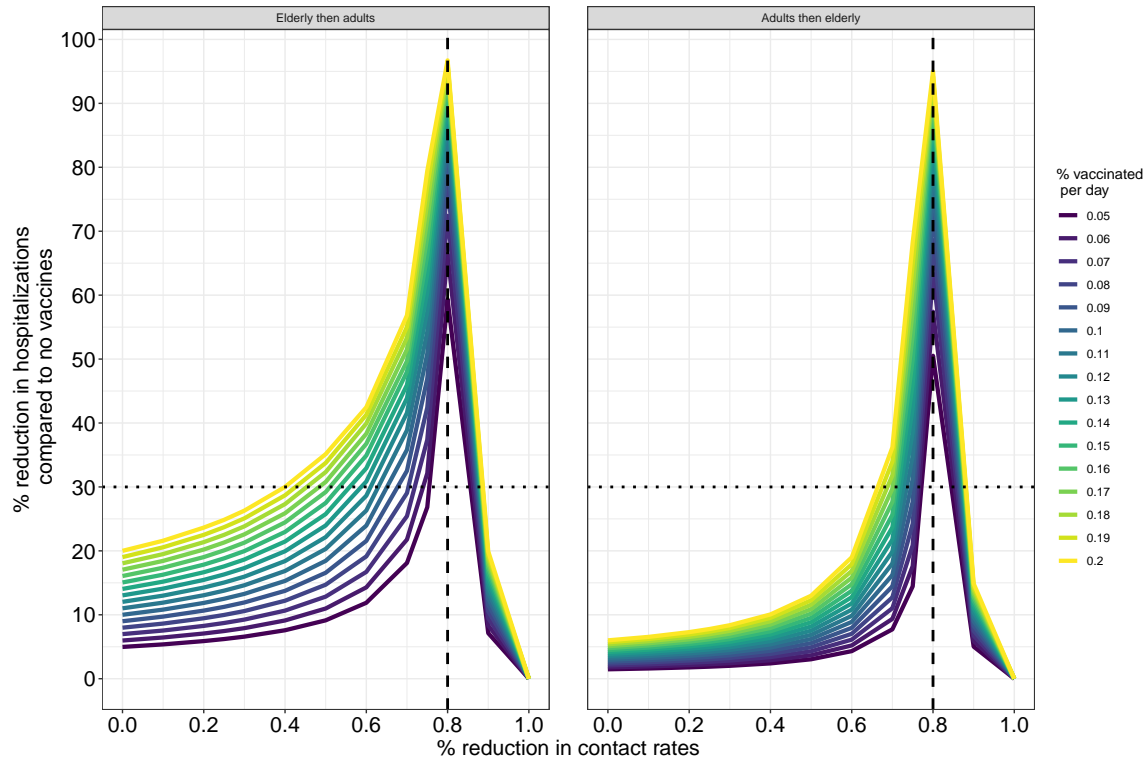


Figure S19: Comparison between prioritization strategies with uniform social distancing. The plot depicts the F_H^{tot} (y-axis) as a function of increasing social distancing (0: no social distancing; 1: no contacts). Line colors depict κ , the proportion of the population vaccinated per day. Two strategies are shown: Vaccinating all elderly (60+) and then all adults (20-59) (left panel); and vaccinating adults and then elderly (right panel). In both strategies there is a threshold of reduction in contacts (dashed vertical line) above which vaccination is no longer effective. Horizontal dotted line provides an example of how the same level of reduction in hospitalizations (here, $F_H^{tot} = 0.3$) can be achieved using different combinations of social distancing, vaccine prioritization and vaccine deployment rates.

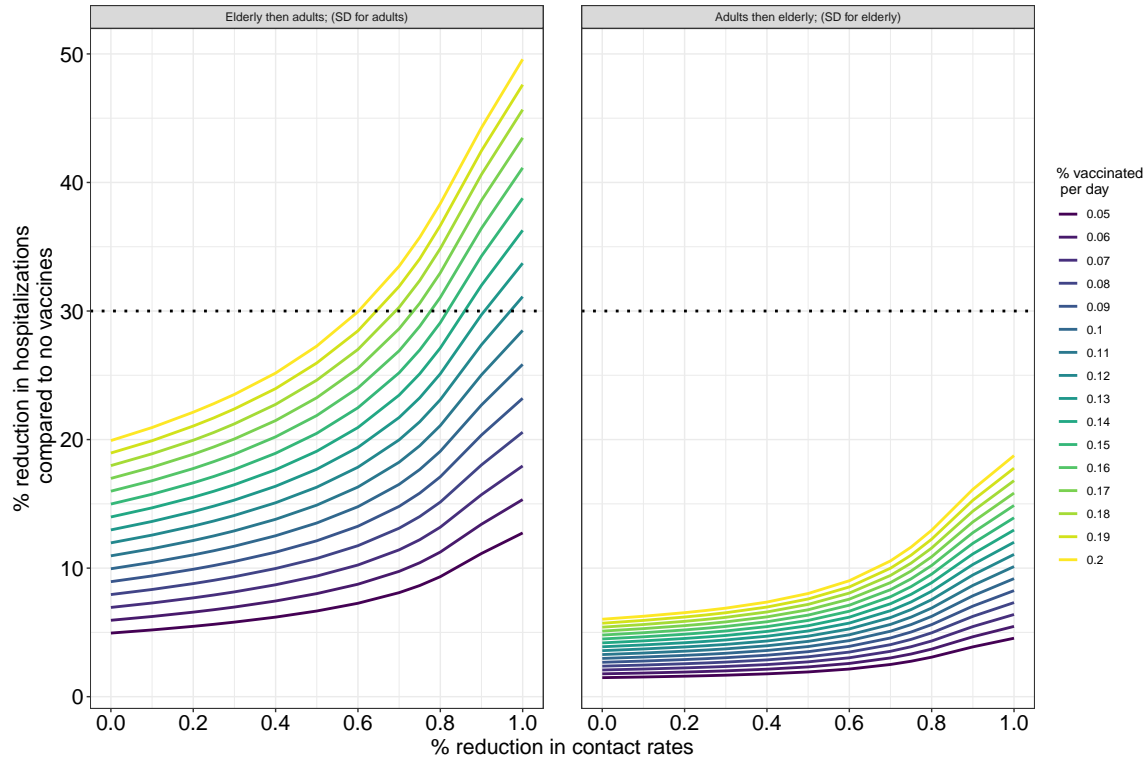


Figure S20: Comparison between prioritization strategies with targeted social distancing. The plot depicts the F_H^{tot} (y-axis) as a function of increasing social distancing (0: no social distancing; 1: no contacts). Line colors depict κ , the proportion of the population vaccinated per day. Two strategies are shown: Vaccinating all elderly (60+) and then all adults (20-59), while applying social distancing only in the adult group (left panel); and vaccinating adults and then elderly, while applying social distancing only in the elderly group (right panel). Horizontal dotted line at $F_H^{tot} = 0.3$ is the same as in Fig. 4 and shows that vaccines has very little in reducing hospitalization when prioritized to adults.

S3.4 Germany

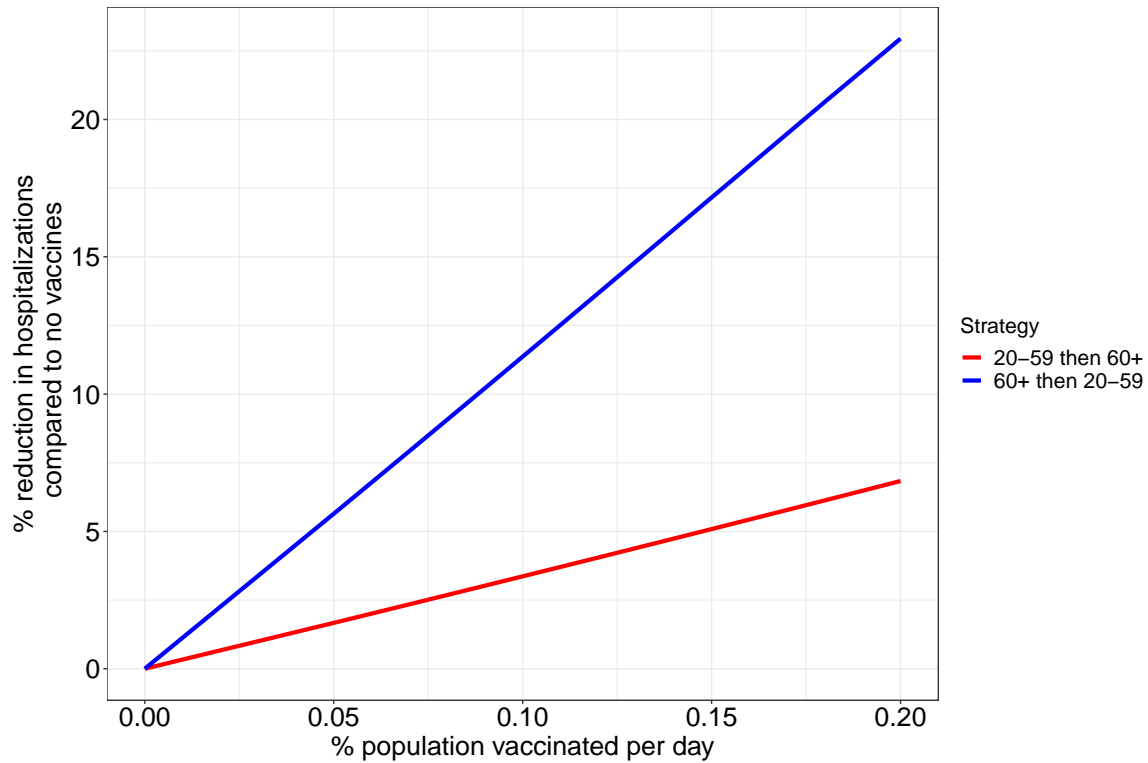


Figure S21: Comparison between prioritization strategies with no social distancing. The plot depicts the F_H^{tot} (y-axis) as a function of increasing vaccination rates (κ), measured as the proportion of the population vaccinated per day. Vaccinating elderly (60+) and then adults (20-59)—depicted in the blue line—is more effective than vaccinating adults and then elderly (red line).

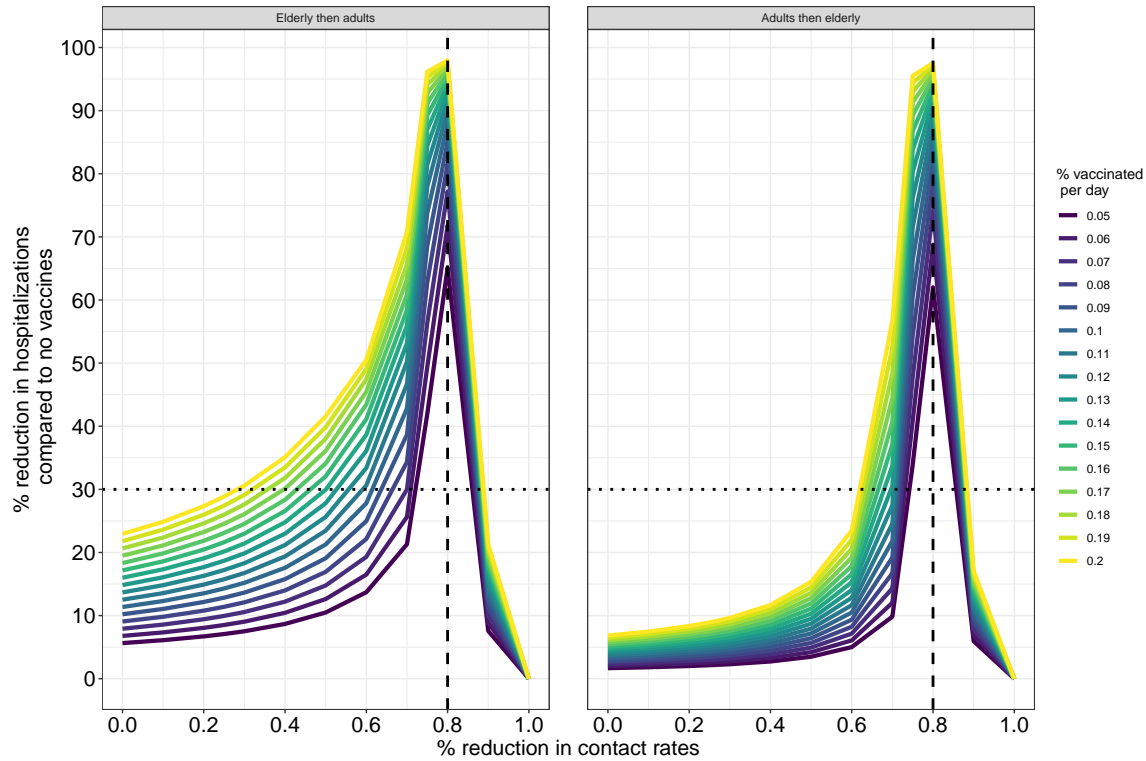


Figure S22: Comparison between prioritization strategies with uniform social distancing. The plot depicts the F_H^{tot} (y-axis) as a function of increasing social distancing (0: no social distancing; 1: no contacts). Line colors depict κ , the proportion of the population vaccinated per day. Two strategies are shown: Vaccinating all elderly (60+) and then all adults (20-59) (left panel); and vaccinating adults and then elderly (right panel). In both strategies there is a threshold of reduction in contacts (dashed vertical line) above which vaccination is no longer effective. Horizontal dotted line provides an example of how the same level of reduction in hospitalizations (here, $F_H^{tot} = 0.3$) can be achieved using different combinations of social distancing, vaccine prioritization and vaccine deployment rates.

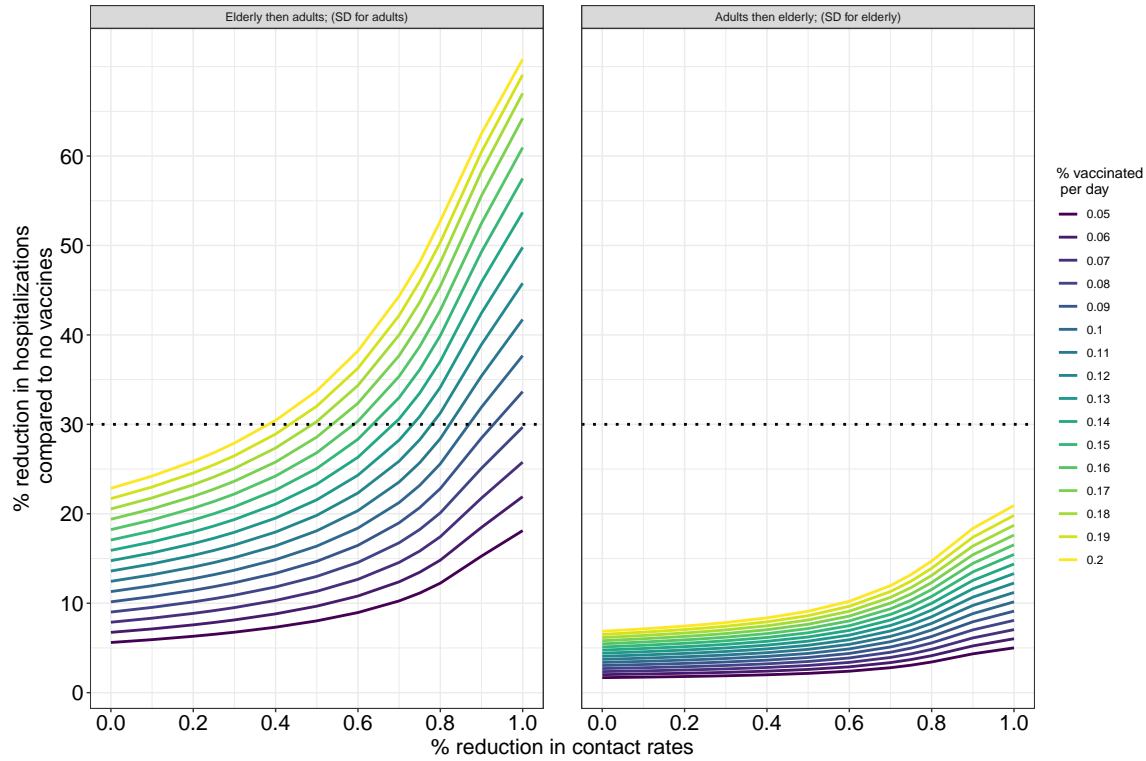


Figure S23: Comparison between prioritization strategies with targeted social distancing. The plot depicts the F_H^{tot} (y-axis) as a function of increasing social distancing (0: no social distancing; 1: no contacts). Line colors depict κ , the proportion of the population vaccinated per day. Two strategies are shown: Vaccinating all elderly (60+) and then all adults (20-59), while applying social distancing only in the adult group (left panel); and vaccinating adults and then elderly, while applying social distancing only in the elderly group (right panel). Horizontal dotted line at $F_H^{tot} = 0.3$ is the same as in Fig. 4 and shows that vaccines has very little in reducing hospitalization when prioritized to adults.

S3.5 Luxembourg

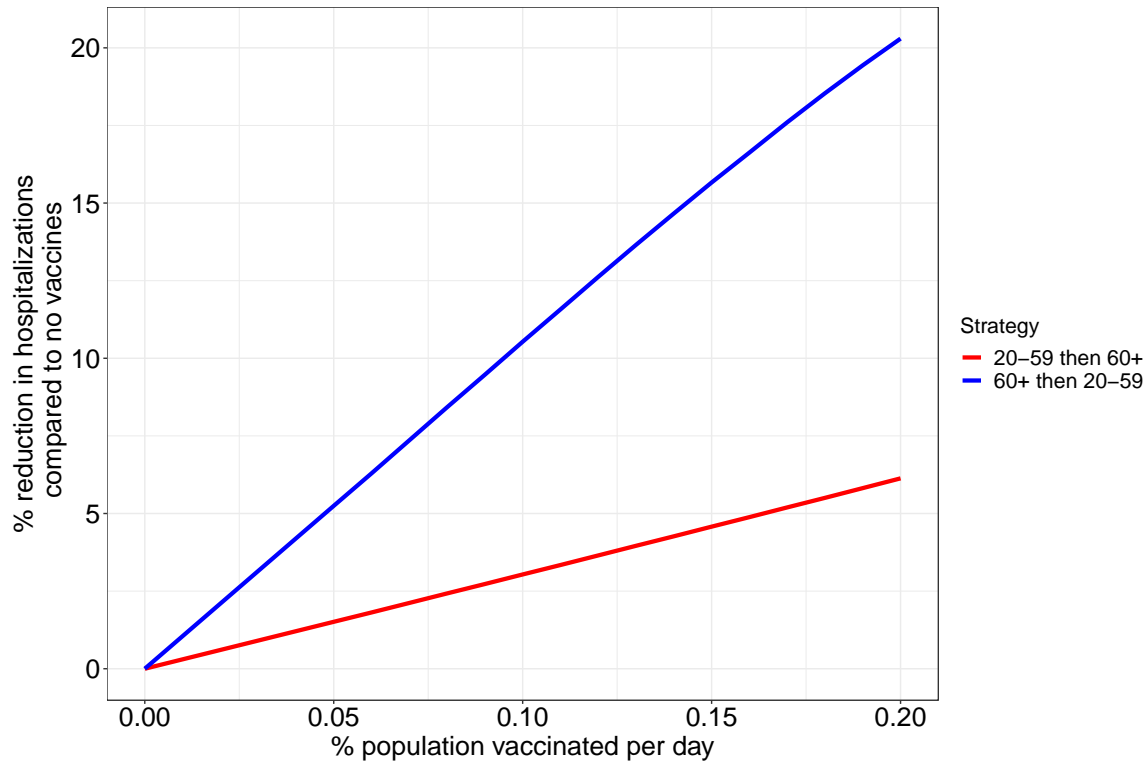


Figure S24: Comparison between prioritization strategies with no social distancing. The plot depicts the F_H^{tot} (y-axis) as a function of increasing vaccination rates (κ), measured as the proportion of the population vaccinated per day. Vaccinating elderly (60+) and then adults (20-59)—depicted in the blue line—is more effective than vaccinating adults and then elderly (red line).

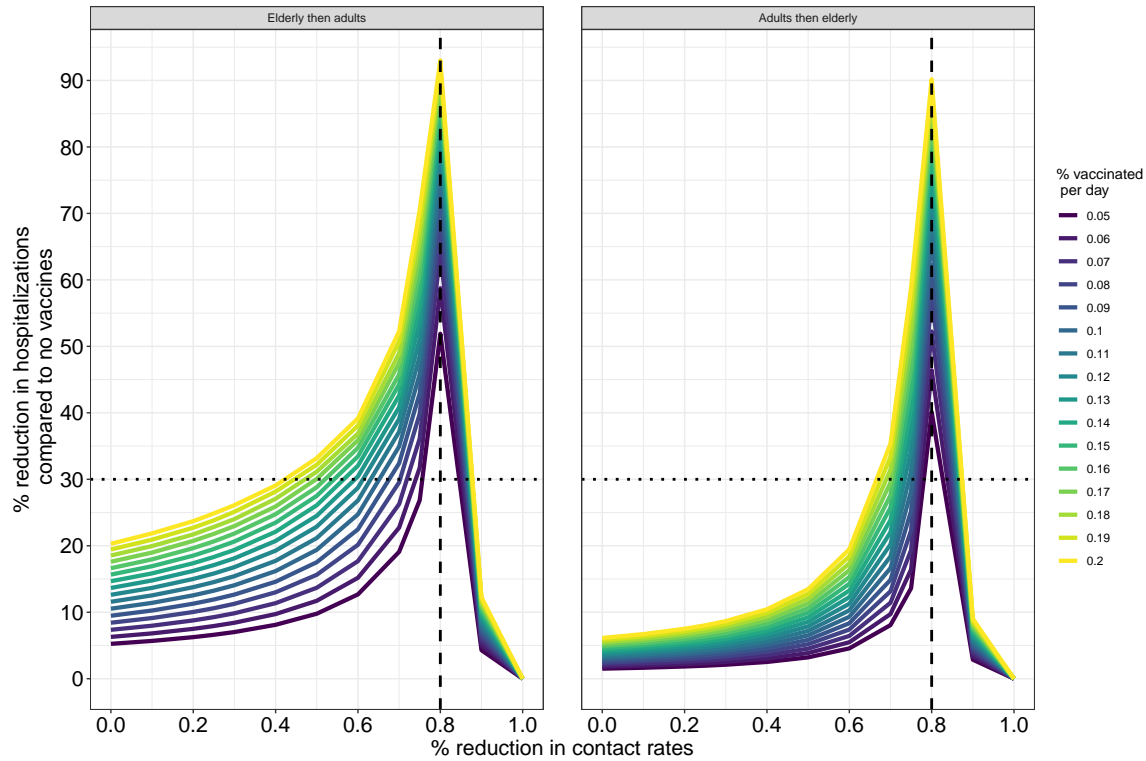


Figure S25: Comparison between prioritization strategies with uniform social distancing. The plot depicts the F_H^{tot} (y-axis) as a function of increasing social distancing (0: no social distancing; 1: no contacts). Line colors depict κ , the proportion of the population vaccinated per day. Two strategies are shown: Vaccinating all elderly (60+) and then all adults (20-59) (left panel); and vaccinating adults and then elderly (right panel). In both strategies there is a threshold of reduction in contacts (dashed vertical line) above which vaccination is no longer effective. Horizontal dotted line provides an example of how the same level of reduction in hospitalizations (here, $F_H^{tot} = 0.3$) can be achieved using different combinations of social distancing, vaccine prioritization and vaccine deployment rates.

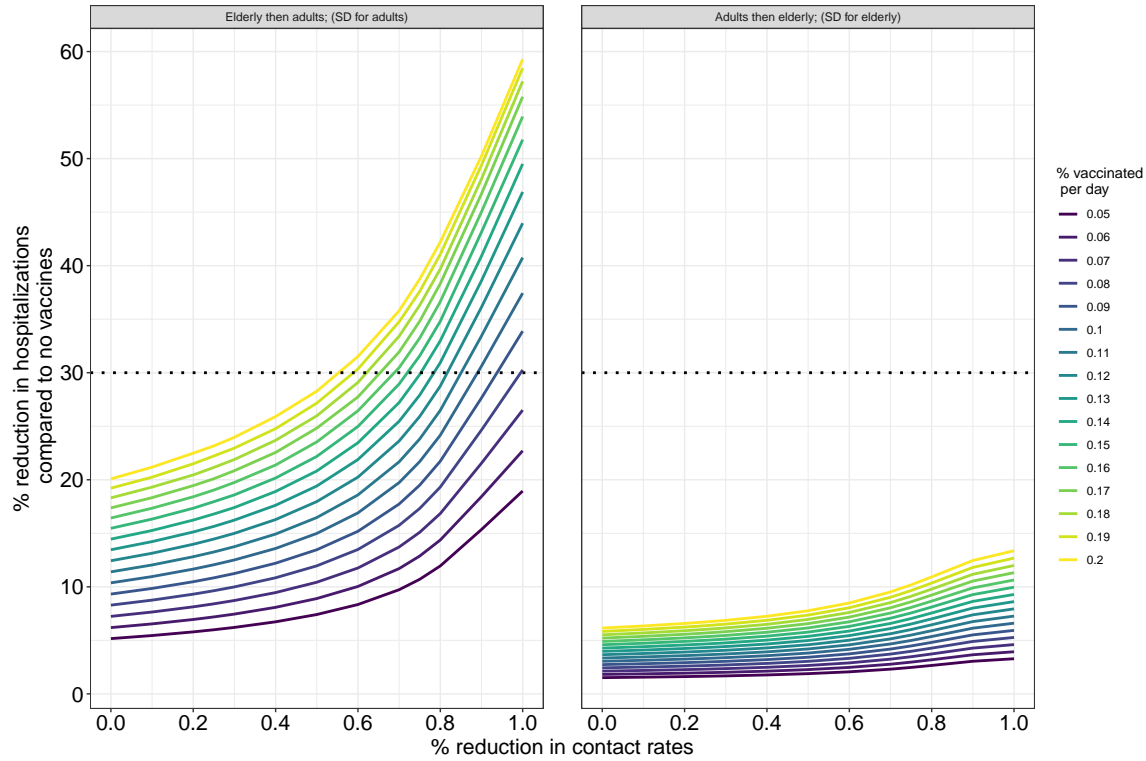


Figure S26: Comparison between prioritization strategies with targeted social distancing. The plot depicts the F_H^{tot} (y-axis) as a function of increasing social distancing (0: no social distancing; 1: no contacts). Line colors depict κ , the proportion of the population vaccinated per day. Two strategies are shown: Vaccinating all elderly (60+) and then all adults (20-59), while applying social distancing only in the adult group (left panel); and vaccinating adults and then elderly, while applying social distancing only in the elderly group (right panel). Horizontal dotted line at $F_H^{tot} = 0.3$ is the same as in Fig. 4 and shows that vaccines has very little in reducing hospitalization when prioritized to adults.